

Optimal Design of Satellite Constellation Configurations with Mixed Integer Linear Programming

David O. Williams Rogers*

West Virginia University, Morgantown, West Virginia, 26506

Dongshik Won[†]

TelePIX, Seoul, 07330, Republic of Korea,

Korea Advanced Institute of Science and Technology, Daejeon 34141, Republic of Korea

Dongwook Koh[‡], and Kyungwoo Hong[§]

TelePIX, Seoul, 07330, Republic of Korea

Hang Woon Lee[¶]

West Virginia University, Morgantown, West Virginia, 26506

Designing satellite constellation systems involves complex multidisciplinary optimization in which coverage serves as a primary driver of overall system cost and performance. Among the various design considerations, constellation configuration—how satellites are placed and distributed in space relative to each other—predominantly determines the resulting coverage. In constellation configuration design, coverage can be considered either as an objective or a constraint, driven by mission objectives. State-of-the-art literature addresses each situation on a case-by-case basis, applying a unique set of assumptions, modeling, and solution methods. Although such a problem-based methodology is valuable, users often face implementation challenges when performing trade-off studies across different mission scenarios, as each scenario must be handled distinctly. In response, we propose a unifying framework consisting of five mixed-integer linear program formulations that are of practical significance, extensible to more complex mission narratives using additional constraints, and capable of obtaining provably optimal constellation configurations. It can handle various metrics and mission scenarios, such as percent coverage, average or maximum revisit times, fixed number of satellites, spatiotemporally varying coverage requirements, and ground-, aerial-, or space-based, static or mobile targets. The paper presents several add-ons, case studies, and comparative analyses to demonstrate the versatility of the proposed framework.

This paper is a substantially revised and expanded version of the Paper AIAA 2023-4658, presented at the 2023 ASCEND, Las Vegas, NV, October 23-25, 2023. It offers new results and a better description of the materials.

*Ph.D. Student, Department of Mechanical, Materials and Aerospace Engineering, Student Member AIAA.

[†]Director, Future Innovation Research Team; Ph.D. Candidate, Department of Aerospace Engineering, Member AIAA.

[‡]Director, Satellite Development Team.

[§]Principal Research Engineer, Future Innovation Research Team

[¶]Assistant Professor, Department of Mechanical, Materials and Aerospace Engineering; hangwoon.lee@mail.wvu.edu. Member AIAA (Corresponding Author).

Nomenclature

\mathcal{J}	=	Set of orbital slots (index j)
\mathcal{P}	=	Set of targets (index p)
\mathcal{T}	=	Mission planning horizon (index t)
\mathbf{b}	=	Coverage timeline
π	=	Observation reward
\mathbf{c}	=	Orbital slot cost
\mathbf{r}	=	Coverage requirement threshold
\mathbf{D}	=	Spatiotemporal coverage parameter
\mathbf{V}	=	Boolean visibility matrix
\mathbf{W}	=	Boolean inter-satellite links matrix
N	=	Number of satellites in the constellation
\mathbf{g}	=	Inter-satellite visibility parameter
ρ	=	Inter-satellite link range
ϵ	=	Inter-satellite link bias parameter
β	=	Small positive real-valued parameter
z	=	Maximum revisit time upper bound parameter
γ	=	Average revisit time upper bound parameter
ΔV	=	Delta-velocity
\mathbf{x}	=	Satellite location decision variable
\mathbf{y}	=	Coverage state decision variable
\mathbf{Z}	=	Maximum revisit time decision variable
ω	=	Length of coverage gap variable
\mathbf{u}	=	Auxiliary variable
\mathbf{i}	=	Coverage gap indicator variable
α	=	Average revisit time upper bound variable
\mathbf{a}	=	Auxiliary decision variable

I. Introduction

Satellite constellations constitute a critical component of spaceborne infrastructure, supporting a wide range of applications in scientific research and civil services, including remote sensing [1–3], telecommunications [4–6], and position, navigation and timing services [7–9]. As distributed systems consisting of multiple satellites, satellite

constellations offer enhanced resilience to individual satellite failures, improved spatiotemporal resolution, and increased overall reliability and mission performance compared to traditional monolithic satellite systems. Recent advancements in deployment technologies, the increased availability of rideshare launch opportunities, and the growing standardization of satellite manufacturing have substantially lowered barriers to space access. These developments have strengthened the case for constellation-based architectures, facilitating the design of more scalable, cost-effective missions and expanding the scope of space-based capabilities.

Designing a satellite constellation system entails a complex optimization process that must account for its inherently interdisciplinary nature, encompassing technical, social, and policy-related dimensions (*e.g.*, spacecraft design, constellation configuration, ground segment, frequency spectrum utilization, decommissioning procedures). These aspects are tightly coupled, necessitating an integrated approach to system design. To this end, the literature often employs multidisciplinary design optimization (MDO) as a structured approach to address interdependencies between system components. MDO is a methodology tailored for optimizing systems composed of multiple interacting disciplines, each with its own local design variables and coupling variables, facilitating information exchange across disciplines and capturing their interrelationships [10]. A system-level optimizer coordinates the individual disciplines, seeking to optimize a global objective while ensuring both system-wide (global) and discipline-specific (local) feasibility constraints are satisfied. For instance, Ref. [11] formulates the conceptual design of a distributed satellite system within a monolithic MDO architecture, where all disciplines are integrated into a single optimization framework. Their formulation simultaneously maximizes the number of images captured and minimizes life-cycle cost. A related study by Ref. [12] adopts a distributed MDO architecture, modeling each discipline as an independent optimization problem. Their objective is to identify a satellite constellation with minimum system mass. Similarly, Ref. [13] utilizes a collaborative optimization technique, a form of distributed MDO, to design satellite constellations by minimizing total system cost. Their formulation incorporates multiple disciplinary domains, including constellation configuration, spacecraft design, and launch scheduling.

Coverage is a fundamental figure of merit in constellation system design due to its direct impact on mission performance and cost. In Earth observation and surveillance missions, coverage determines the amount of data that can be collected from targets, whereas in telecommunications, it governs the number of users served and the quality of service provided. These requirements are jointly characterized by the geographical region of interest—regional or global—and the desired temporal resolution—continuous or discontinuous. In particular, for discontinuous coverage, performance is typically evaluated using metrics such as percentage coverage, maximum revisit time (MRT)—the longest coverage gap between successive observations—and average revisit time (ART)—the mean coverage gaps between observations [14]. The coverage delivered by the constellation depends on various factors, for instance, the payload characteristics (*e.g.*, remote sensing sensors or communications’ antennas) and their control subsystem (*e.g.*, if the satellite can perform slewing maneuvers), the number of satellites and their orbits, and exogenous factors (*e.g.*,

cloud coverage). Among the various factors involved, the constellation configuration, which encompasses the number of satellites, their geometric arrangement, and their orbital characteristics, plays a central role in determining the coverage delivered by the system [12, 13]. As such, the design of constellation configurations that consider coverage as a key performance metric, whether treated as an objective (*e.g.*, maximizing percentage coverage or minimizing ART) or as a constraint (*e.g.*, minimizing the number of satellites required for continuous coverage), constitutes a critical challenge in the literature, due to its strong correlation with both mission effectiveness and cost-efficiency.

The literature sheds light on the value of constellation configuration design and optimization with coverage as the figure of merit, however, a significant research gap remains unaddressed. Specifically, the literature adopts global, regional, continuous, and discontinuous coverage as the optimization’s figures of merit. These efforts are reviewed in detail in Sec. I.A, and as an overview, modeling techniques predominantly consist of geometrical and nonlinear models and integer linear programming (ILP) formulations. Further, the approaches taken to optimize the design of constellation configurations are based on brute force, heuristics, metaheuristics, and exact algorithms. Hence, it is clear that there is no unified framework for modeling and solving constellation configuration design problems. Consequently, the available literature proposes problem-specific approaches to design optimal constellation configurations addressing different spatiotemporal coverage requirements.

In response to this gap, we propose a unified optimization framework, consisting of five elementary formulations, each of which tackles a figure of merit of coverage, facilitating the complex task of designing constellation configurations. Specifically, this paper reviews two existing formulations from the literature and proposes three novel ones. All formulations are mixed-integer linear programming problems (MILP) at large, enabling the user to obtain provably optimal solutions, for a defined set of discrete candidate orbits, through the use of commercial solvers (*e.g.*, branch and bound). The formulations are general enough to address complex spatiotemporal coverage requirements for single or multiple static and dynamic targets, and the resulting constellation configurations are not constrained to follow specific (a-)symmetrical distributions. Furthermore, three of the five formulations are a one-to-one resemblance to specific facility location problem (FLP) formulations from operations research. The first formulation, originally proposed in Ref. [15], is equivalent to the set covering location problem (SCLP) [16], and determines the minimum cost constellation configuration that delivers continuous coverage over the regions of interest. The second formulation resembles the partial set covering location problem (PSCLP) [16], and retrieves the minimum cost constellation configuration that delivers at least D percentage coverage over the regions of interest. The third formulation, firstly introduced in Ref. [17], adopts the maximal covering location problem (MCLP) formulation [18], and finds the optimal constellation configuration that uses exactly N satellites that maximizes the percentage coverage over the regions of interest. The fourth formulation, the minimal maximum revisit time problem (MMRT), minimizes the MRT over the targets by determining the optimal constellation configuration that uses exactly N satellites. Similarly, the fifth formulation, the minimal average revisit time problem (MART), minimizes the ART over the specified targets by determining the optimal N satellite constellation

configuration.

In addition to the five formulations described above, we expand the applicability of SCLP to further mission scenarios, considering different design requirements by proposing a set of add-ons. First, we incorporate robust inter-satellite links (ISL) into the constellation configuration design by adding a set of additional constraints inspired by Dirac’s theorem, a theorem from graph theory that enforces a cycle that visits all nodes in the graph (*i.e.*, Hamiltonian cycle). Second, instead of imposing a continuous coverage requirement, we impose an upper bound on the MRT during the constellation configuration design using a set of MMRT constraints. Third, we design a minimum cost constellation configuration that has an upper bound on the ART over the targets by leveraging constraints originally devised for MART. The contributions of this paper, as well as the constellation configuration design flow, are illustrated in Fig. 1. Specifically, given a set of targets, either static or dynamic, the user defines if the coverage is a requirement or the objective, and selects the corresponding formulation. The outcome of the optimization problem is the optimal constellation configuration that complies with the coverage specifications over the desired targets.

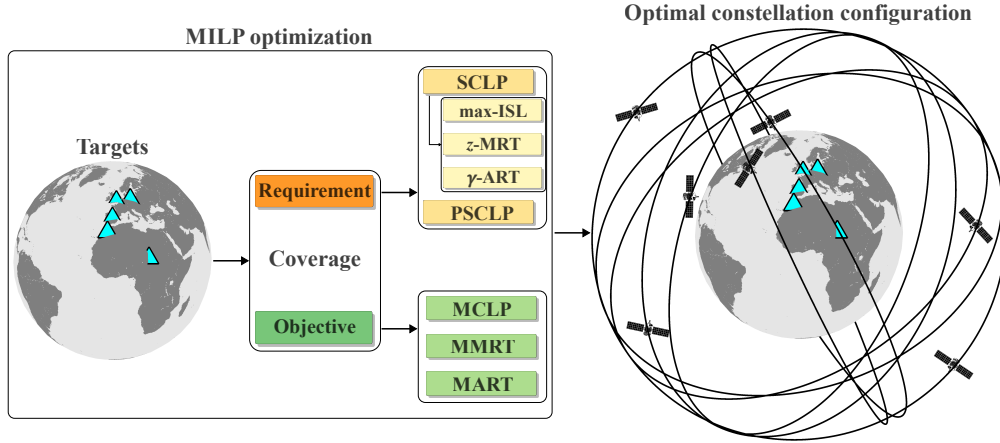


Fig. 1 Constellation configuration design procedure and optimization formulations proposed in this paper.

The remainder of this paper is organized as follows. Section I.A reviews existing methods for constellation configuration design. Section II introduces the optimization parameters and presents the five MILP formulations, each illustrated with a corresponding example. Section III describes the SCLP add-ons, compares the fundamental formulations, and includes case studies that highlight additional applications. Finally, Section IV summarizes the main findings and outlines directions for future research.

A. Literature Review

This section reviews state-of-the-art methodologies for constellation configuration design. For selected studies, we highlight, where applicable, their key assumptions, modeling approaches, and solution methods. For simplicity, we organize the review by global or regional, and by continuous or discontinuous coverage; the review is not necessarily mutually exclusive and may not be fully comprehensive.

The literature proposes different approaches to tackle the problem of constellation configuration design for global coverage. For instance, geometrical arguments and enumeration procedures are used to design constellation configurations where all satellites are placed in circular orbits with common altitude, uniform distribution of the orbital planes' right ascension of the ascending node (RAAN) along the reference plane, and common inclination, *e.g.*, Walker Delta patterns [19, 20], and Rosette [21] with inclined orbits, and configurations as in Ref. [22] with polar orbits. Further, if the RAAN's distribution is constrained to half of the equatorial plane, and all orbits share a pair of intersection points lying on the reference plane, the constellation configuration corresponds to Walker Star patterns [19]. Similar geometrical relations are used to determine constellation configurations that use polar orbits to provide n -fold coverage with the minimum number of satellites [23, 24]. Conversely, an optimization approach based on genetic algorithms (GA) is proposed in Ref. [25] to design multilayer constellation configurations consisting of two Walker Delta patterns to increase the robustness against satellite failures. The 2D lattice flower constellations (2D LFC), a constellation pattern with common semi-major axis, eccentricity, and inclination, and with mean anomaly and RAAN satisfying specific geometrical relationships, are posed as an alternative for global coverage [26]. Expanding 2D LFC, the authors in Ref. [27] achieve global symmetry and uniform spacing for elliptical orbits to deliver global coverage by incorporating into the design space the J_2 perturbation. Moreover, multi-layer constellation configuration design for telecommunications services are proposed using a gradient descent-based algorithm [28], and a heuristic algorithm [29].

Constellation configuration design for covering specific regions of the globe, *i.e.*, regional coverage, is tackled by the literature with multiple approaches. Geometrical relations solved through enumeration procedures are used to obtain constellation configuration to deliver n -fold coverage over specific regions of interest, assuming circular [30], polar [23], and elliptical orbits [31] with a uniform distribution of satellites. Further, simulation-based methods are employed to design Walker Delta patterns [32, 33] and asymmetrical constellation configurations [33]. In addition, optimization formulations that model the problem of constellation configuration design are considered. For instance, a multi-objective optimization problem that minimizes the maximum orbital altitude and the number of satellites using elliptical orbits to deliver polar coverage over the Moon is proposed in Ref. [34] and solved using GA. Conversely, Ref. [15] proposes a single-objective ILP and obtains optimal constellation configurations using repeating ground track (RGT) orbits for Earth regional coverage.

The literature adopts a wide range of approaches for designing constellation configurations for continuous coverage. For instance, Walker patterns aim to deliver continuous global coverage, and their design relies on geometrical arguments and enumeration procedures [19, 20]. In addition, iterative computational procedures are used to solve the coverage geometrical formulations to design minimal constellation configurations with polar orbits [35]. Centering on regional coverage, Ref. [36] proposes the geometrical design of satellite constellation configurations using Molniya orbits. Further, nonlinear optimization models are solved using commercial solvers to determine minimal constellation configurations adopting polar orbits or Walker Delta patterns [37]. Similarly, a sequential design procedure that relies on nonlinear

models and optimization is used to design constellation configurations that adopt frozen tundra orbits [38]. These are elliptical orbits with geosynchronous periods, and where at least one orbital element does not vary significantly over time [38]. Further, GA is proposed to solve a multi-objective optimization formulation intended to design a constellation configuration for regional coverage, considering the number of satellites, their visibility, and their orbital altitude [39]. In contrast, Ref. [15] designs constellation configurations that deliver continuous coverage leveraging ILP formulations.

Likewise, several design approaches are adopted for designing constellation configurations by defining as figure of merit the three categories of discontinuous coverage. For instance, Ref. [40] tackles the design of constellation configurations with discontinuous coverage over geographical regions prone to hurricanes using a multi-objective optimization formulation and solves it through a state-of-the-art nonlinear commercial solver. Conversely, Ref. [17] tackles the design of constellation configurations maximizing the percentage coverage, over any region of interest, by proposing an ILP formulation and solving it using a commercial optimization solver. Similarly, Ref. [41] maximizes the percentage coverage over multiple targets, proposing the flower constellations, characterized by having repeating ground track orbits and specific phasing rules. Adopting the MRT as the design metric, Ref. [32] proposes an enumeration-based procedure to obtain constellation configurations with an upper-bound on the MRT following Walker Delta patterns. Further, a multi-objective optimization, solved through a Non-dominated Sorting Genetic Algorithm II (NSGA-II), is proposed to obtain constellation configurations that minimize the MRT at the expense of image quality [42]. In addition to optimizing for the MRT as the sole discontinuous coverage metric, multi-objective optimization formulations are used to concurrently minimize the ART and MRT. In particular, optimized constellation configurations are obtained by solving the optimization problem using GA [43], and NSGA-II [44].

Significant efforts have been made in the literature to develop design (optimization) methods for determining optimal satellite constellation configurations. However, to the best of the authors' knowledge, existing approaches remain highly problem-specific. Most studies focus on a particular coverage-related figure of merit, leading to differing fundamental assumptions, modeling strategies, and solution techniques. This fragmentation highlights a critical gap in the literature and serves as the primary motivation for this work. In this paper, we propose a unified MILP framework that presents formulations we believe are both practically critical and sufficiently distinct to warrant recognition as a unique formulation in their most basic form, as evidenced by existing literature. The goal is for the proposed framework to provide users with a go-to reference for easy implementation via commercial off-the-shelf solvers (*e.g.*, CPLEX and Gurobi Optimizer), while offering a desirable property (*i.e.*, certificate of optimality).

II. Constellation Configuration Design Optimization Problem Formulations

This section begins by introducing the general notation and definitions common to all formulations. Subsequently, we present each MILP formulation accompanied by an illustrative example. All formulations are solved to optimality.

A. Notation and Definitions

We define the following general sets, parameters, and decision variables applicable to all problems discussed in this paper. A summary is provided in Table 1. Definitions specific to individual problems will be addressed in their respective subsections.

Let \mathcal{T} denote the set of discrete uniform time steps, with index t and cardinality T . The cardinality of the set denotes the number of time steps. Let \mathcal{J} denote the set of orbital slots, with index j and cardinality J . Each orbital slot j is characterized by its initial position and velocity vectors defined at the epoch t_1 . Further, each orbital slot is associated with a cost parameter $c_j \in \mathbb{R}_{\geq 0}$, for all $j \in \mathcal{J}$. The cost parameter can be defined differently for various mission scenarios, aiming to capture specific features. For instance, c_j could represent the cost of deploying a satellite to orbital slot j , or it could signify the station-keeping cost associated with that orbital slot during the mission.

We define \mathcal{P} as the set of targets, with index p and cardinality P . Each target can be static (*e.g.*, a ground station) or dynamic (*e.g.*, an airplane, ship, spacecraft). Each target p has an associated latitude, longitude, and elevation at each time step t , in addition to a time-dependent coverage requirement r_{tp} such that r_{tp} is a positive integer greater than unity. That is, we say that target p is covered if and only if it is visible to at least r_{tp} satellites at time step t . The significance of parameter r_{tp} is that it provides flexibility to the user to specify multi-fold, time-varying coverage requirements during the entire mission or specific time windows.

The Boolean visibility parameter $V \in \{0, 1\}^{T \times J \times P}$ encodes the visibility of orbital slots over the set of targets during the mission horizon and is defined as:

$$V_{tjp} = \begin{cases} 1, & \text{if target } p \text{ is visible to orbital slot } j \text{ at time step } t \\ 0, & \text{otherwise} \end{cases}$$

To construct V , we propagate orbital slot j using its initial position and velocity vectors, as defined at epoch t_1 , throughout the mission planning horizon. At each time step, we apply visibility masking and encode the corresponding Boolean visibility state V_{tjp} . The use of a Boolean parameter to encode visibility states allows the user to select any desired orbital propagator and to adopt either custom or commercial off-the-shelf satellite-target access computation algorithms.

In this paper, we present a collection of mathematical formulations to tackle various constellation configuration design optimization problems in MILP fashion. All problems are built on the concept of orbital slots and share binary decision variables x_j , defined as:

$$x_j = \begin{cases} 1, & \text{if orbital slot } j \text{ is taken by a satellite} \\ 0, & \text{otherwise} \end{cases}$$

It is assumed that satellites do not change orbital slots during the mission time horizon. The optimal decision variable vector \mathbf{x}^* (where the asterisk indicates optimality), also referred to as optimal constellation pattern vector, is the set of orbital slots occupied by satellites and is a subset of \mathcal{J} . Consequently, \mathbf{x}^* is used to construct the optimal constellation configuration.

Table 1 General sets, parameters, and variables for the MILP formulations.

Type	Symbol	Description
Sets	\mathcal{J}	Set of orbital slots (index j ; cardinality J)
	\mathcal{P}	Set of targets (index p ; cardinality P)
	\mathcal{T}	Set of time steps (index t ; cardinality T)
Parameters	c_j	Generic cost parameter for orbital slot j ($c_j \in \mathbb{R}_{\geq 0}$)
	r_{tp}	Generic coverage threshold for target p at time step t ($r_{tp} \in \mathbb{Z}_{\geq 1}$)
	V_{tjp}	$\begin{cases} 1, & \text{if orbital slot } j \text{ is visible from target point } p \text{ at time step } t \\ 0, & \text{otherwise} \end{cases}$
Decision variables	x_j	$\begin{cases} 1, & \text{if a satellite occupies orbital slot } j \\ 0, & \text{otherwise} \end{cases}$

B. Illustrative Example Parameters

We present illustrative examples to help readers visualize the objective of each formulation better, particularly in comparing the resultant constellation pattern vectors relative to one another. To clearly emphasize the differences among the five fundamental formulations, all examples adhere to the same set of problem parameters. We solve each formulation using the Gurobi optimizer version 12.0.2 with default settings. Note that all illustrative examples can be solved using other off-the-shelf solvers such as CPLEX or MATLAB's `intlinprog`.

Each illustrative example consists of 287 time steps of size 5 min, with an epoch defined as January 1, 2025, at 12:00:00.000 Universal Coordinated Time (UTC). San Diego, California, USA (geodetic coordinates 32.71°N, 117.16°W) is designated as the sole target with the coverage requirement parameter set as $r_{tp} = 1$ for all $t \in \mathcal{T}$, and a minimum elevation angle of 5 deg. Without loss of generality and for ease of exposition, we assume that orbital slots are placed in circular RGT orbits. These orbits repeat their ground track with a period of repetition that depends on the time between two successive RAAN crossings along the prime meridian, denoted as the Greenwich period, the time interval between two crossings of the satellite through the orbit's RAAN, and the RAAN and argument of latitude are constrained to satisfy specific relations [15]. We adopt a 12:1 resonance (12 revolutions in one nodal period of Greenwich), a period of repetition of 86,399.34 s, a semi-major axis of 8054.57 km, and an inclination of 102.9 deg. These assumptions enable us to present the results as prescribed by the access-pattern-coverage (APC) decomposition [15]. To this end, we adopt two additional vectors defined in the APC decomposition: the reference visibility profile \mathbf{v} and the coverage

timeline \mathbf{b} . The reference visibility profile \mathbf{v} encodes the coverage state of the reference satellite that uniquely defines the visibility matrix \mathbf{V} . The coverage timeline \mathbf{b} characterizes the coverage state of the optimal constellation throughout each target's mission planning horizon. Mathematically, \mathbf{V} , \mathbf{x} , and \mathbf{b} are interrelated as a linear system, expressed by:

$$\mathbf{b} = \mathbf{V}\mathbf{x} \quad (1)$$

where all illustrative examples have the same \mathbf{V} while yielding different \mathbf{x} , resulting in different coverage timelines. It is noteworthy to mention that Eq. (1) can be utilized to compute the coverage timeline of constellation configurations using non-RGT orbits, on the condition that the visibility parameter \mathbf{V} can be computed.

C. Set Covering Location Problem

The binary integer linear programming formulation [15] based on the APC decomposition technique resembles the SCLP formulation from FLP. In the context of constellation configuration design optimization, SCLP determines the minimum cost constellation configuration that strictly satisfies the complex spatiotemporal coverage requirements. The total cost of the configuration is encoded in objective function (2).

$$\sum_{j \in \mathcal{J}} c_j x_j \quad (2)$$

The spatiotemporal coverage requirement over the set of targets is enforced with constraints (3), given as:

$$\sum_{j \in \mathcal{J}} V_{tjp} x_j \geq r_{tp}, \quad \forall t \in \mathcal{T}, \forall p \in \mathcal{P} \quad (3)$$

Piecing it all together, the mathematical formulation of SCLP is as follows [15]:

$$\text{(SCLP)} \quad \min \quad \sum_{j \in \mathcal{J}} c_j x_j \quad (2)$$

$$\text{s.t.} \quad \sum_{j \in \mathcal{J}} V_{tjp} x_j \geq r_{tp}, \quad \forall t \in \mathcal{T}, \forall p \in \mathcal{P} \quad (3)$$

$$x_j \in \{0, 1\}, \quad \forall j \in \mathcal{J} \quad (4)$$

Example 1 (Single-fold Continuous Coverage SCLP). We present the design of an optimal constellation configuration for continuous coverage with the parameters defined in Sec. II.B. The optimal constellation has 20 satellites. Figure 2a presents the APC decomposition [15]. At the top of it lies the visibility profile of the seed satellite, at the middle the constellation pattern vector, which indicates the selected orbital slots, and at the bottom is the coverage timeline of the optimal constellation. Figure 2b presents the distribution of all orbital slots in the RAAN versus argument of latitude

plane, and the selected orbital slots are indicated with red squares. Lastly, Fig. 2c presents a 3D visualization with the satellites, their orbits in the Earth-centered inertial (ECI) frame, and the target.

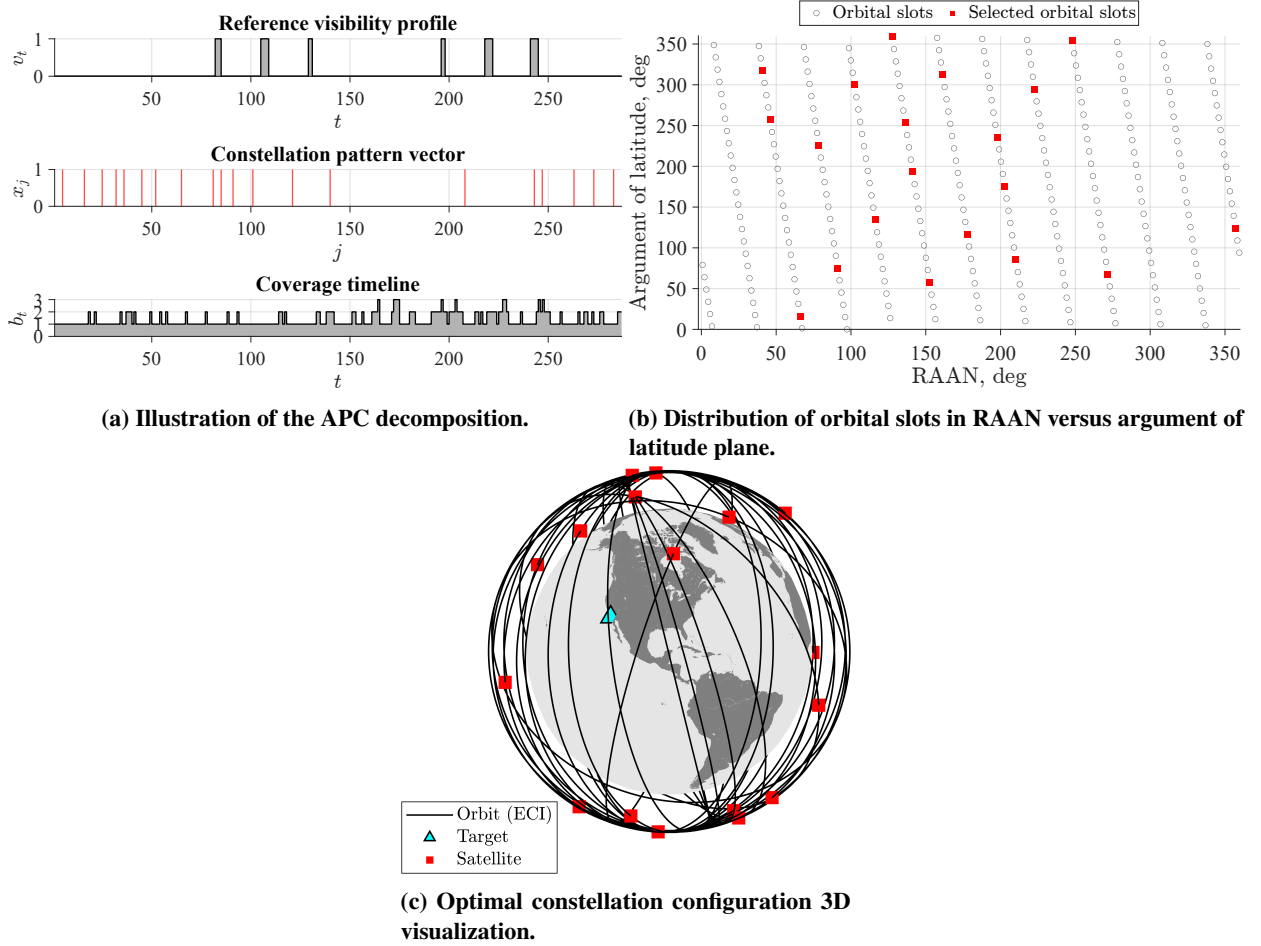


Fig. 2 SCLP formulation results.

D. Partial Set Covering Location Problem

In the context of satellite constellation design, PSCLP, originally devised as a class of FLP, seeks to determine the minimum cost constellation configuration such that at least the minimum temporal *percentage coverage* requirement over each target is satisfied at the minimum cost. The PSCLP formulation holds practical importance as it allows mission designers to implement the concept of temporal percentage coverage, a universally adopted figure of merit in constellation design and analysis [45].

PSCLP generalizes SCLP by incorporating more flexible coverage requirements. Unlike SCLP, which seeks to fully satisfy the continuous coverage requirements imposed on all target points, PSCLP permits partial fulfillment of these coverage requirements, hence percentage coverage. This added flexibility enables PSCLP to be better suited for scenarios where continuous, full coverage is impractical or unnecessary. Table 2 presents additional parameters and

variables used in PSCLP.

Table 2 Specific PSCLP parameters and decision variables.

Type	Symbol	Description
Parameters	D_p	Temporal percentage coverage parameter for target p ($D_p \in [0, T]$)
	D	Spatiotemporal percentage coverage parameter ($D \in [0, T \times P]$)
Decision variables	y_{tp}	$\begin{cases} 1, & \text{if target } p \text{ is covered at time step } t \\ 0, & \text{otherwise} \end{cases}$

Similarly to SCLP, PSCLP seeks to minimize the total cost of the constellation configuration, hence, it adopts objective function (2). To extend the novel temporal percentage coverage requirements, PSCLP leverages Boolean decision variables y_{tp} , defined as:

$$y_{tp} = \begin{cases} 1, & \text{if target } p \text{ is covered at time step } t \\ 0, & \text{otherwise} \end{cases}$$

Constraints (5) and (6) enforce the constellation to achieve at least D_p percentage coverage over each target $p \in \mathcal{P}$.

$$\sum_{j \in \mathcal{J}} V_{tjp} x_j \geq r_{tp} y_{tp}, \quad \forall t \in \mathcal{T}, \forall p \in \mathcal{P} \quad (5)$$

$$\sum_{t \in \mathcal{T}} y_{tp} \geq D_p, \quad \forall p \in \mathcal{P} \quad (6)$$

It is important to highlight that if $D_p = T$ for all $p \in \mathcal{P}$, we are imposing full coverage as a requirement, and this formulation resembles SCLP. Lastly, the extended mathematical formulation for PSCLP is given as:

$$\text{(PSCLP)} \quad \min \quad \sum_{j \in \mathcal{J}} c_j x_j \quad (2)$$

$$\text{s.t.} \quad \sum_{j \in \mathcal{J}} V_{tjp} x_j \geq r_{tp} y_{tp}, \quad \forall t \in \mathcal{T}, \forall p \in \mathcal{P} \quad (5)$$

$$\sum_{t \in \mathcal{T}} y_{tp} \geq D_p, \quad \forall p \in \mathcal{P} \quad (6)$$

$$x_j \in \{0, 1\}, \quad \forall j \in \mathcal{J} \quad (4)$$

$$y_{tp} \in \{0, 1\}, \quad \forall t \in \mathcal{T}, \forall p \in \mathcal{P} \quad (7)$$

Remark 1 (Mean Percent Coverage). A variation of this formulation is possible if, instead of setting individual temporal percent coverage requirements as in constraints (6) per target p , one may impose a *mean spatiotemporal percent coverage*

requirement D , where D can be obtained by taking the mean of D_p for all p in \mathcal{P} . In this case, constraints (6) would be replaced by the following constraint:

$$\sum_{p \in \mathcal{P}} \sum_{t \in \mathcal{T}} y_{tp} \geq D$$

Example 2 (Single-fold 80 % Coverage). Given a required minimum percentage coverage of 80 % and the parameters defined in Sec. II.B, the optimal constellation configuration has 13 satellites. The optimal constellation delivers a percentage coverage of 80.13 % over San Diego. Figure 3a presents the APC decomposition, and Fig. 3b outlines the distribution of the orbital slots in the RAAN versus argument of latitude plane. Figure 3c illustrates a 3D visualization of the constellation configuration and the target.

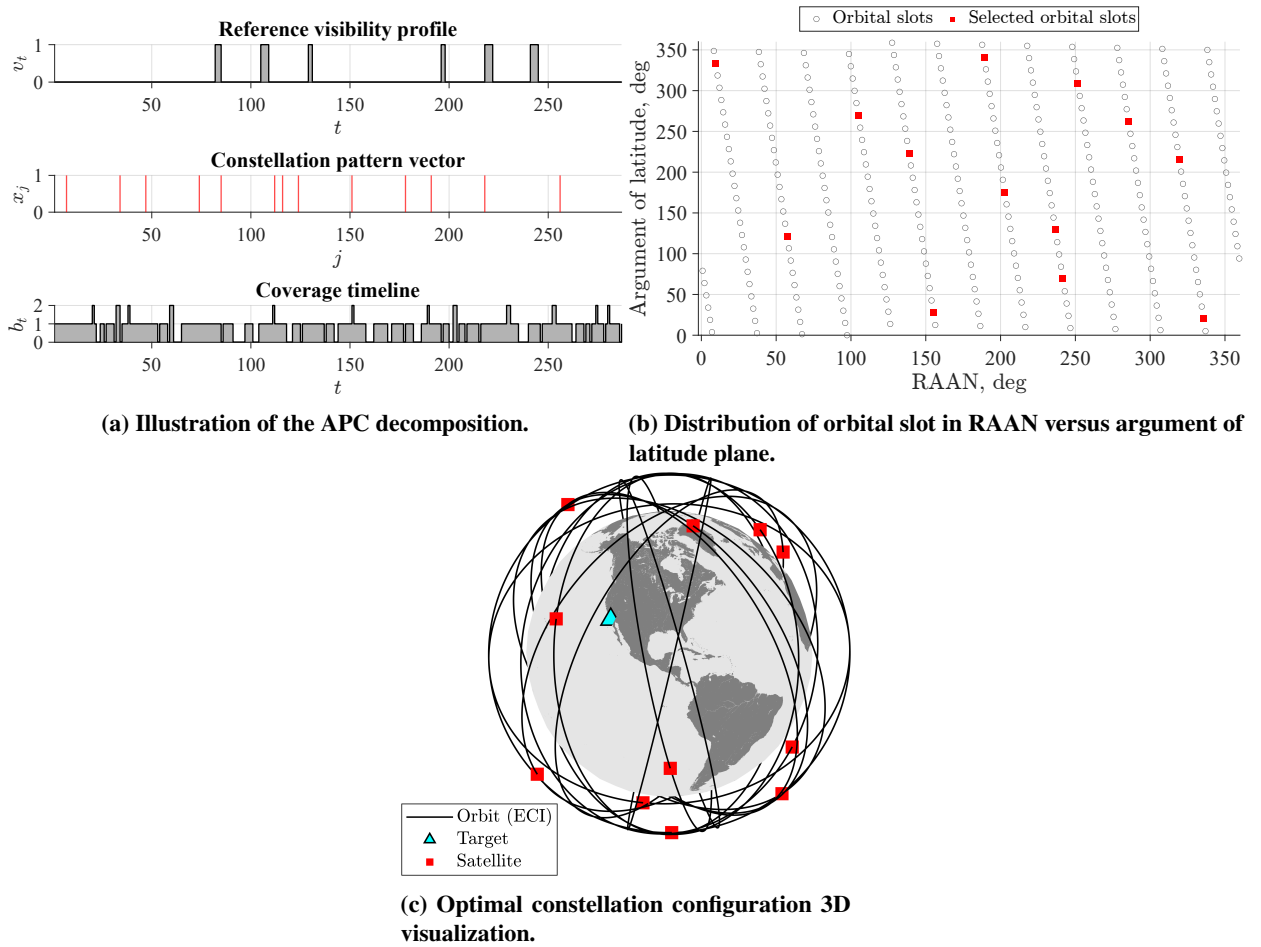


Fig. 3 PSCLP formulation results.

E. Maximal Covering Location Problem

The MCLP, also known as the maximum coverage problem, originally introduced in Ref. [17], seeks to locate N satellites within a set \mathcal{J} to maximize the sum of time-dependent observation rewards associated with a target. The

significance of MCLP applied to the constellation configuration design optimization is that it enables the user to design a constellation where the number of satellites to be used is a parameter and the objective is to obtain the maximum observational rewards over a set of targets. This objective is distinctive from those of SCLP and PSCLP, which seek to provide continuous coverage or a percentage D_p of coverage over the targets while considering the number of satellites as a decision variable instead of a parameter. Table 3 presents the parameters specific to MCLP.

Table 3 Specific MCLP parameters.

Type	Symbol	Description
Parameters	π_{tp}	Observation reward for target p at time step t ($\pi_{tp} \in \mathbb{R}_{\geq 0}$)
	N	Number of satellites in the constellation

The objective of MCLP is to maximize the sum of the time-dependent observation rewards over the set of targets, given as:

$$\sum_{p \in \mathcal{P}} \sum_{t \in \mathcal{T}} \pi_{tp} y_{tp} \quad (8)$$

where π_{tp} encodes the observation reward associated to target p at time step t and is collected if the target is covered. The coverage state of each target is enforced by constraints (5).

The constellation is enforced to use exactly N satellites with the cardinality constraint defined as:

$$\sum_{j \in \mathcal{J}} x_j = N \quad (9)$$

Integrating the objective function and constraints, the MCLP formulation is as follows:

$$\text{(MCLP)} \quad \max \quad \sum_{p \in \mathcal{P}} \sum_{t \in \mathcal{T}} \pi_{tp} y_{tp} \quad (8)$$

$$\text{s.t.} \quad \sum_{j \in \mathcal{J}} V_{tjp} x_j \geq r_{tp} y_{tp}, \quad \forall t \in \mathcal{T}, \forall p \in \mathcal{P} \quad (5)$$

$$\sum_{j \in \mathcal{J}} x_j = N \quad (9)$$

$$x_j \in \{0, 1\}, \quad \forall j \in \mathcal{J} \quad (4)$$

$$y_{tp} \in \{0, 1\}, \quad \forall t \in \mathcal{T}, \forall p \in \mathcal{P} \quad (7)$$

Remark 2 (MCLP with Constellation Cost). In certain mission design scenarios, it is more useful to limit the maximum cost of the satellite constellation instead of fixing the number of satellites. In such cases, one can replace constraint (9)

with constraints:

$$\sum_{j \in \mathcal{J}} c_j x_j \leq C \quad (10)$$

where C is the maximum cost of the constellation.

Example 3 (12-satellite MCLP). Fixing the number of satellites to 12, the optimal constellation configuration delivers 78.04 % coverage over San Diego. The APC decomposition for the optimal constellation is depicted in Fig. 4a, and the orbital slot distribution in the RAAN versus argument of latitude plane in Fig. 4b. Figure 4c presents the optimal constellation configuration and San Diego.

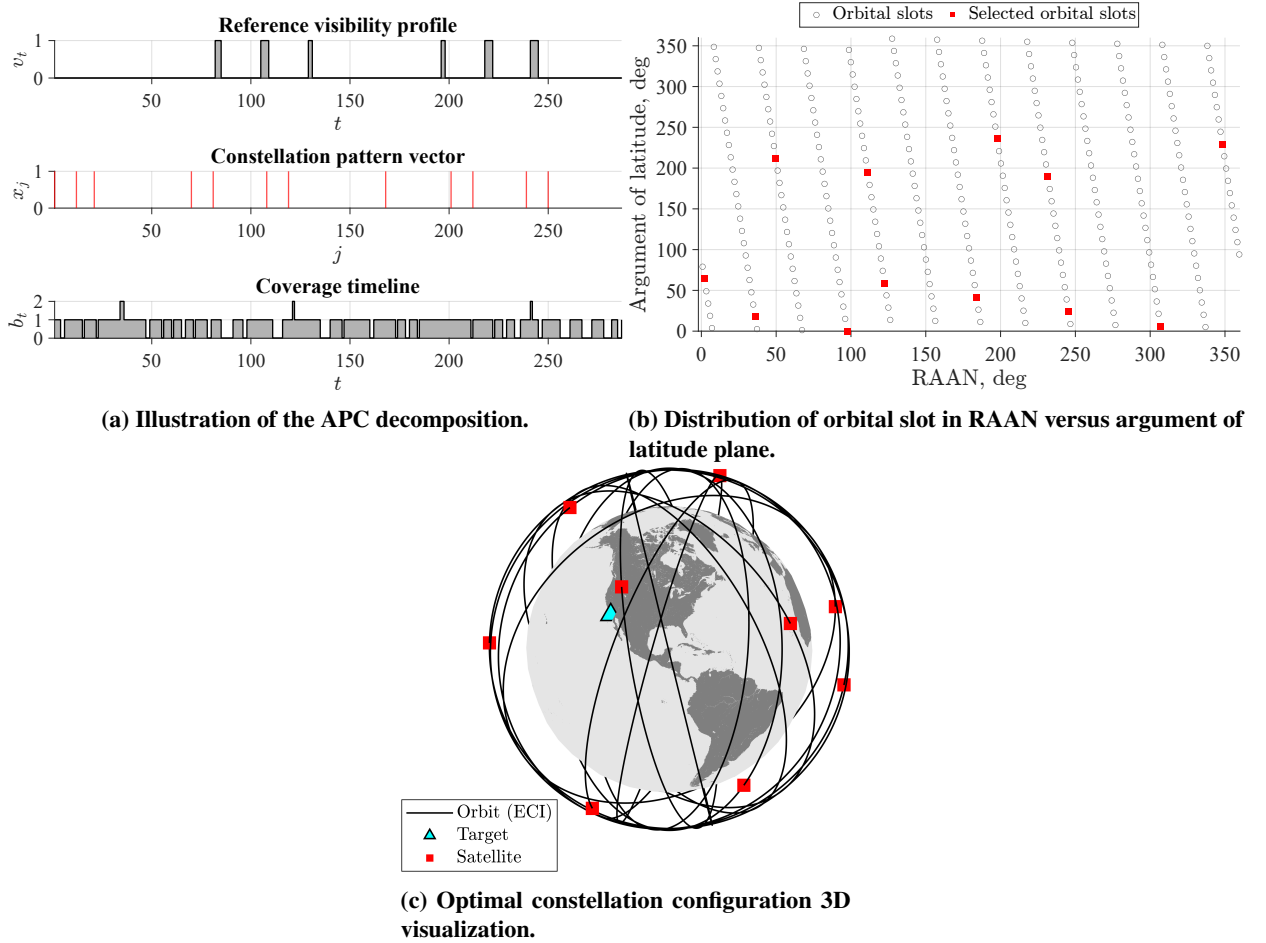


Fig. 4 MCLP formulation results.

F. Minimal Maximum Revisit Time Problem

MMRT aims to determine the location of N satellites to minimize the MRT . This formulation is a minimax optimization problem given its objective. The MRT is an important metric for Earth observation missions (*e.g.*, surveillance, disaster monitoring) and communication services where the maximum length of the coverage gaps impacts

the performance of the mission. Even though this formulation fixes the number of satellites to be used, it is different from MCLP in the sense that it focuses on the length of the coverage gaps instead of maximizing the coverage *per se*. Table 4 introduces the novel decision variables used in the formulation.

Table 4 Specific MMRT parameters and decision variables.

Type	Symbol	Description
Parameter	β	Small positive real-valued auxiliary parameter ($\beta \in \mathbb{R}_{>0}$)
Decision variables	ω_{tp}	Length of coverage gap at time step t for target p ($\omega_{tp} \in [0, T]$)
	Z	Integer variable representing the MRT ($Z \in [0, T]$)
	u_p	Auxiliary variable for target p ($u_p \in [0, T]$)

The objective of this formulation is to minimize the MRT encoded in decision variable Z , given cardinality constraints (9). To determine if a target is covered or not, we leverage the big-M method and introduce coverage constraints given as:

$$\sum_{j \in \mathcal{J}} V_{tjp} x_j - r_{tp} \geq -T(1 - y_{tp}) - \beta, \quad \forall t \in \mathcal{T}, \forall p \in \mathcal{P} \quad (11)$$

$$\sum_{j \in \mathcal{J}} V_{tjp} x_j - r_{tp} \leq T y_{tp} - \beta, \quad \forall t \in \mathcal{T}, \forall p \in \mathcal{P} \quad (12)$$

where β is a small positive real-valued constant.

As the interest of the formulation is to minimize the MRT, new auxiliary decision variables are introduced. ω_{tp} is a nonnegative integer variable that encodes the revisit time of the constellation by counting the number of contiguous time steps where target p is not covered until time step t . Constraints (13) initialize decision variable $\omega_{1,p}$ considering the coverage state at the first time step for each target p . If a target is covered at time step t , constraints (14) enforce ω_{tp} to zero. Alternatively, if the target is not covered, *i.e.*, $y_{tp} = 0$, constraints (14) are nonbinding and constraints (15) and (16) yield an equality increasing the value of $\omega_{t-1,p}$ by one. Further, constraints (17) couple the MRT with the largest gap encoded by ω_{tp} .

$$\omega_{1,p} = 1 - y_{1,p}, \quad \forall p \in \mathcal{P} \quad (13)$$

$$\omega_{tp} \leq T(1 - y_{tp}), \quad \forall t \in \mathcal{T}, \forall p \in \mathcal{P} \quad (14)$$

$$\omega_{tp} - \omega_{t-1,p} \leq 1, \quad \forall t \in \mathcal{T} \setminus \{1\}, \forall p \in \mathcal{P} \quad (15)$$

$$\omega_{tp} - \omega_{t-1,p} \geq 1 - T y_{tp}, \quad \forall t \in \mathcal{T} \setminus \{1\}, \forall p \in \mathcal{P} \quad (16)$$

$$\omega_{tp} \leq Z, \quad \forall t \in \mathcal{T}, \forall p \in \mathcal{P} \quad (17)$$

$$\omega_{tp} \geq 0, \quad \forall t \in \mathcal{T}, \forall p \in \mathcal{P} \quad (18)$$

In summary, the MMRT formulation is given as:

$$\text{(MMRT)} \quad \min \quad Z \quad (19)$$

$$\text{s.t.} \quad \sum_{j \in \mathcal{J}} x_j = N \quad (9)$$

$$\sum_{j \in \mathcal{J}} V_{tjp} x_j - r_{tp} \geq -T(1 - y_{tp}) - \beta, \quad \forall t \in \mathcal{T}, \forall p \in \mathcal{P} \quad (11)$$

$$\sum_{j \in \mathcal{J}} V_{tjp} x_j - r_{tp} \leq T y_{tp} - \beta, \quad \forall t \in \mathcal{T}, \forall p \in \mathcal{P} \quad (12)$$

$$\omega_{1,p} = 1 - y_{1,p}, \quad \forall p \in \mathcal{P} \quad (13)$$

$$\omega_{tp} \leq T(1 - y_{tp}), \quad \forall t \in \mathcal{T}, \forall p \in \mathcal{P} \quad (14)$$

$$\omega_{tp} - \omega_{t-1,p} \leq 1, \quad \forall t \in \mathcal{T} \setminus \{1\}, \forall p \in \mathcal{P} \quad (15)$$

$$\omega_{tp} - \omega_{t-1,p} \geq 1 - T y_{tp}, \quad \forall t \in \mathcal{T} \setminus \{1\}, \forall p \in \mathcal{P} \quad (16)$$

$$\omega_{tp} \leq Z, \quad \forall t \in \mathcal{T}, \forall p \in \mathcal{P} \quad (17)$$

$$\omega_{tp} \geq 0, \quad \forall t \in \mathcal{T}, \forall p \in \mathcal{P} \quad (18)$$

$$x_j \in \{0, 1\}, \quad \forall j \in \mathcal{J} \quad (4)$$

$$y_{tp} \in \{0, 1\}, \quad \forall t \in \mathcal{T}, \forall p \in \mathcal{P} \quad (7)$$

Remark 3 (Cyclic Property). If the coverage timelines of all orbital slots are guaranteed to be repeated over the specified mission planning horizon, as in the case specified in Ref. [15], then the first and last time steps of the optimization problem are coupled, yielding a circularity in the visibility profile. To account for this property, constraints (13) are replaced by constraints (20a) to (20e) to link the first and last time steps.

$$\omega_{1,p} = \omega_{T,p} + 1 - y_{1,p} - u_p, \quad \forall p \in \mathcal{P} \quad (20a)$$

$$u_p \leq T y_{1,p}, \quad \forall p \in \mathcal{P} \quad (20b)$$

$$u_p \leq \omega_{T,p}, \quad \forall p \in \mathcal{P} \quad (20c)$$

$$u_p \geq \omega_{T,p} - T(1 - y_{1,p}), \quad \forall p \in \mathcal{P} \quad (20d)$$

$$u_p \geq 0, \quad \forall p \in \mathcal{P} \quad (20e)$$

Remark 4 (Minimizing the Sum of MRTs). If, instead of minimizing the MRT of the entire set of targets, the user seeks to minimize the sum of each target's MRT, certain modifications have to be made. First, constraints (17) are replaced by constraints (22) such that the MRT decision variable is defined for each target. Second, objective function (19) is

substituted by objective function (21), which encodes the sum of the MRTs.

$$\sum_{p \in \mathcal{P}} Z_p \quad (21)$$

$$\omega_{tp} \leq Z_p, \quad \forall t \in \mathcal{T}, \forall p \in \mathcal{P} \quad (22)$$

Example 4 (12-satellite MMRT). The 12-satellite optimal constellation configuration has an objective value Z of 3, and an MRT of 15 min. The constellation's APC decomposition is presented in Fig. 5a, and the orbital slots' spatial distribution in Fig. 5b. The optimal constellation configuration as well as the target are illustrated in Fig. 5c.

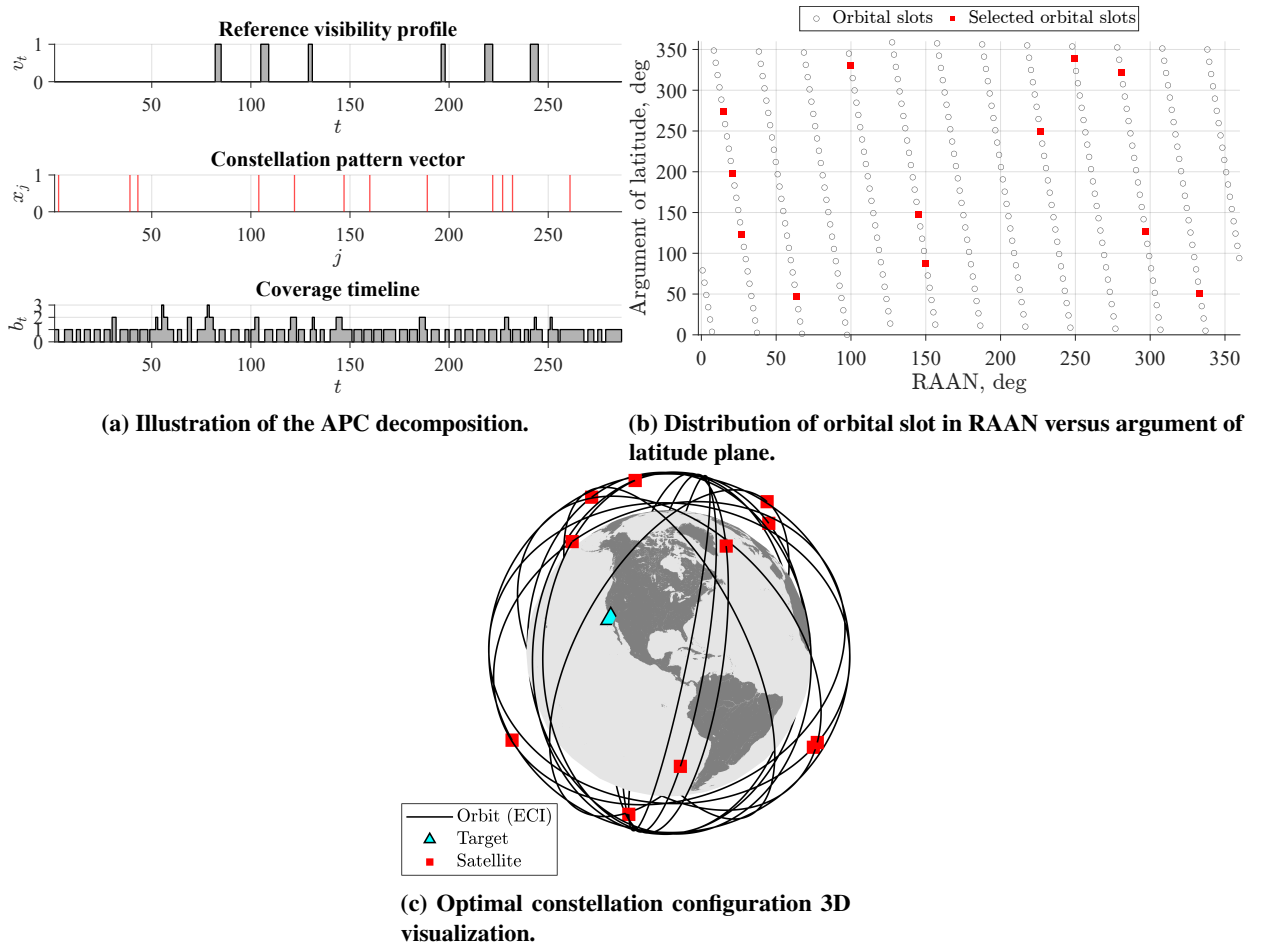


Fig. 5 MMRT formulation results.

G. Minimal Average Revisit Time Problem

MART determines the location of N satellites to minimize the ART. The ART metric is paramount in satellite constellation missions where its success and performance depend on the average length of the coverage gaps. The ART

is different from MCLP and MMRT in the sense that it solely focuses on the ART and not on the total coverage or the maximum length of a coverage gap. Table 5 lists the decision variables specific to ART.

Table 5 Specific MART decision variables.

Type	Symbol	Description
Decision variables	i_{tp}	$\begin{cases} 1, & \text{if coverage gap starts at time step } t \text{ for target } p \\ 0, & \text{otherwise} \end{cases}$
	α_p	Upper bound of target p 's ART ($\alpha_p \in \mathbb{R}_{\geq 0}$)
	a_{tp}	Auxiliary variable for target p at time step t ($a_{tp} \in \mathbb{R}_{\geq 0}$)

Decision variables x_j determine the location of the N satellites, and decision variables y_{tp} encode if a target is covered, with their domains defined in constraints (4) and (7), respectively. Additionally, to encode the start of a coverage gap during the mission, we propose the following gap indicator decision variables:

$$i_{tp} = \begin{cases} 1, & \text{if a coverage gap starts at time step } t \text{ for target } p \\ 0, & \text{otherwise} \end{cases}$$

The ART is defined as the summation of all coverage gaps divided by the number of gaps, mathematically defined as:

$$\text{ART} = \sum_{p \in \mathcal{P}} \frac{T - \sum_{t \in \mathcal{T}} y_{tp}}{\sum_{t \in \mathcal{T}} i_{tp}} \quad (23)$$

The objective function that minimizes the sum of α_p for all $p \in \mathcal{P}$ is given as:

$$\sum_{p \in \mathcal{P}} \alpha_p \quad (24)$$

where Eq. (24) is the upper bound of the ART:

$$\sum_{p \in \mathcal{P}} \alpha_p \geq \sum_{p \in \mathcal{P}} \frac{T - \sum_{t \in \mathcal{T}} y_{tp}}{\sum_{t \in \mathcal{T}} i_{tp}} \quad (25)$$

Letting a_{tp} be a nonlinear auxiliary variable that relates the start of a coverage gap with the ART, defined as:

$$a_{tp} = \alpha_p i_{tp} \quad (26)$$

which additionally couples, for each time step t and for each target p , the left-hand side with the denominator in the right-hand side of Eq. (25). Further, we linearize this variable through the Big-M method by tightening the Big-M

parameter to T as:

$$a_{tp} \leq T i_{tp}, \quad \forall t \in \mathcal{T}, \forall p \in \mathcal{P} \quad (27a)$$

$$a_{tp} \leq \alpha_p, \quad \forall t \in \mathcal{T}, \forall p \in \mathcal{P} \quad (27b)$$

$$a_{tp} \geq \alpha_p - T(1 - i_{tp}), \quad \forall t \in \mathcal{T}, \forall p \in \mathcal{P} \quad (27c)$$

where the motivation for linearizing these variables stems from modeling the ART as an MILP objective function. Then, we couple auxiliary variables a_{tp} with the nominator of Eq. (23) with constraints (28).

$$\sum_{t \in \mathcal{T}} a_{tp} \geq T - \sum_{t \in \mathcal{T}} y_{tp}, \quad \forall p \in \mathcal{P} \quad (28)$$

Constraints (11) and (12) encode each target's coverage state at each time step. At the epoch, constraints (29) couple the coverage state of a target with the gap indicator decision variables.

$$i_{1,p} \leq 1 - y_{1,p}, \quad \forall p \in \mathcal{P} \quad (29)$$

Gap indicator decision variables i_{tp} encode the start of a coverage gap leveraging the big-M method. If a target is covered, constraints (30a) require that gap indicator decision variables i_{tp} are zero. Conversely, constraints (30b) enforce gap indicator decision variables i_{tp} to be one if a coverage gap starts. Further, constraints (30c) enforce decision variables i_{tp} to zero inside a coverage gap.

$$i_{tp} \leq T(1 - y_{tp}), \quad \forall t \in \mathcal{T} \setminus \{1\}, \forall p \in \mathcal{P} \quad (30a)$$

$$i_{tp} \geq y_{t-1,p} - T y_{tp}, \quad \forall t \in \mathcal{T} \setminus \{1\}, \forall p \in \mathcal{P} \quad (30b)$$

$$i_{tp} \leq y_{t-1,p} + y_{tp}, \quad \forall t \in \mathcal{T} \setminus \{1\}, \forall p \in \mathcal{P} \quad (30c)$$

Lastly, piecing all constraints and the objective function together, the MART formulation is given as:

$$\text{(MART)} \quad \min \quad \sum_{p \in \mathcal{P}} \alpha_p \quad (24)$$

$$\text{s.t.} \quad \sum_{j \in \mathcal{J}} x_j = N \quad (9)$$

$$\sum_{j \in \mathcal{J}} V_{tjp} x_j - r_{tp} \geq -T(1 - y_{tp}) - \beta, \quad \forall t \in \mathcal{T}, \forall p \in \mathcal{P} \quad (11)$$

$$\sum_{j \in \mathcal{J}} V_{tjp} x_j - r_{tp} \leq T y_{tp} - \beta, \quad \forall t \in \mathcal{T}, \forall p \in \mathcal{P} \quad (12)$$

$$a_{tp} \leq T i_{tp}, \quad \forall t \in \mathcal{T}, \forall p \in \mathcal{P} \quad (27a)$$

$$a_{tp} \leq \alpha_p, \quad \forall t \in \mathcal{T}, \forall p \in \mathcal{P} \quad (27b)$$

$$a_{tp} \geq \alpha_p - T(1 - i_{tp}), \quad \forall t \in \mathcal{T}, \forall p \in \mathcal{P} \quad (27c)$$

$$\sum_{t \in \mathcal{T}} a_{tp} \geq T - \sum_{t \in \mathcal{T}} y_{tp}, \quad \forall p \in \mathcal{P} \quad (28)$$

$$i_{1p} \leq 1 - y_{1,p}, \quad \forall p \in \mathcal{P} \quad (29)$$

$$i_{tp} \leq T(1 - y_{tp}), \quad \forall t \in \mathcal{T} \setminus \{1\}, \forall p \in \mathcal{P} \quad (30a)$$

$$i_{tp} \geq y_{t-1,p} - T y_{tp}, \quad \forall t \in \mathcal{T} \setminus \{1\}, \forall p \in \mathcal{P} \quad (30b)$$

$$i_{tp} \leq y_{t-1,p} + y_{tp}, \quad \forall t \in \mathcal{T} \setminus \{1\}, \forall p \in \mathcal{P} \quad (30c)$$

$$x_j \in \{0, 1\}, \quad \forall j \in \mathcal{J} \quad (4)$$

$$y_{tp} \in \{0, 1\}, \quad \forall t \in \mathcal{T}, \forall p \in \mathcal{P} \quad (7)$$

$$i_{tp} \in \{0, 1\}, \quad \forall t \in \mathcal{T}, \forall p \in \mathcal{P} \quad (31)$$

Remark 5 (Cyclic Property). To incorporate the circularity in the coverage profile of constellation configurations, constraints (29) are replaced by:

$$i_{1,p} \leq T(1 - y_{1,p}), \quad \forall p \in \mathcal{P} \quad (32a)$$

$$i_{1,p} \geq y_{T,p} - T y_{1,p}, \quad \forall p \in \mathcal{P} \quad (32b)$$

$$i_{1,p} \leq y_{T,p} + y_{1,p}, \quad \forall p \in \mathcal{P} \quad (32c)$$

where the new constraints couple the gap indicator decision variables between the first and last time step for constraints (30a), (30b), and (30c).

Example 5 (12-satellite MART). Forcing a constellation configuration with 12 satellites, MART retrieves an objective

value of 1.39, corresponding to an ART of 6.95 min. Figure 6a presents the APC decomposition for the optimal constellation, Fig. 6b the orbital slots distribution in the RAAN versus argument of latitude plane, and Fig. 6c the 3D visualization of the constellation configuration and the target.

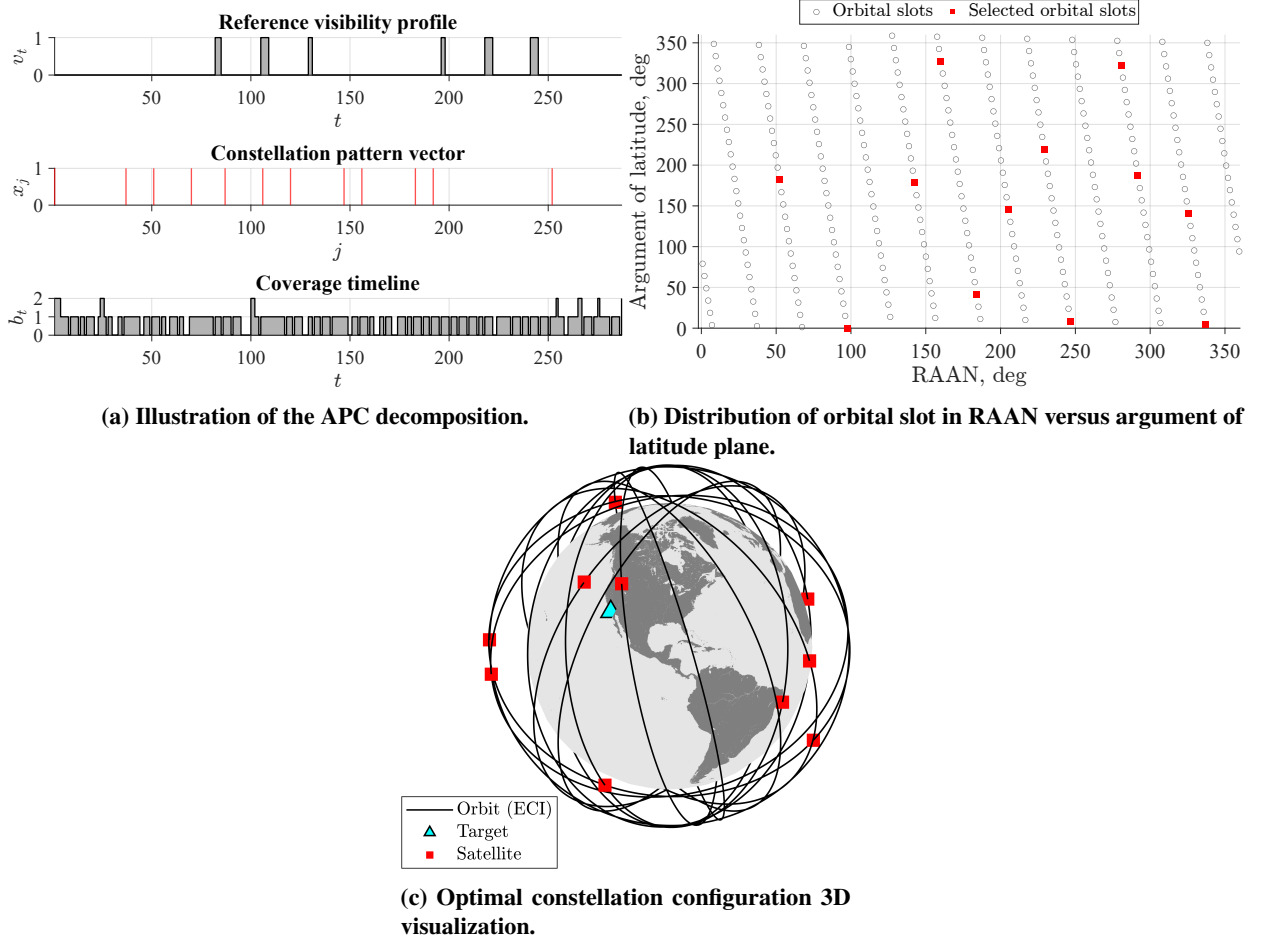


Fig. 6 MART formulation results.

III. Comparative Analyses, Add-Ons, and Case Studies

This section begins by presenting comparative analyses to demonstrate the difference in the optimization objectives and constraints, and, consequently, the results obtained for each formulation. Then, we propose a set of add-ons for the SCLP formulation to consider further mission design specifications and demonstrate the modularity of MILP formulations by interchanging different sets of constraints originally devised for other problems. It is important to note that the add-ons can be proposed for the other formulations, and further mission specifications can be modeled. Lastly, we present two case studies to showcase further applications of the MILP formulations. Specifically, we design a constellation configuration to cover both static and dynamic targets, and a minimum deployment cost constellation configuration.

A. Comparative Analyses of the Five Elementary Formulations

This section aims to demonstrate the difference in the results obtained by each formulation in Sec. II. To this end, we perform two comparisons. First, we compare the number of satellites and the delivered coverage for SCLP, PSCLP, and MCLP. The purpose of this comparative analysis is to provide evidence of the direct relationship between the number of satellites and the percentage coverage delivered by the constellation. Second, we compare the discontinuous coverage figures of merit, *i.e.*, percent coverage, MRT, and ART, obtained by MCLP, MMRT, and MART. This comparison seeks to showcase the influence of orbital distribution while fixing the number of satellites in the discontinuous coverage metrics. Table 6 presents a review of the features considered in each formulation, discriminating them either as an optimization objective or constraints.

Table 6 Optimization objectives and constraints summary for MILP formulations.

Optimization	Figure of merit	SCLP	PSCLP	MCLP	MMRT	MART
Objective	Cost min.	×	×			
	Pct. coverage max.			×		
	MRT min.				×	
	ART min.					×
Constraints	No. of sats.			×	×	×
	Pct. coverage	×	×			

Table 7 presents the number of satellites and the delivered coverage of the optimal constellations obtained by SCLP, PSCLP, and MCLP. The green colored cells indicate the objective of the optimization. The SCLP-based constellation requires 20 satellites to deliver continuous coverage, while the PSCLP-based one requires 13 satellites to deliver at least 80 % coverage, indicating that the 20 % difference is achieved by adding seven satellites to the constellation. Furthermore, the results obtained by PSCLP and MCLP show a drop in coverage close to 2 % by removing one satellite from the constellation.

Table 7 Comparison between SCLP, PSCLP, and MCLP results.

Metric	SCLP	PSCLP	MCLP
Number of satellites	20	13	12 (req. 12)
Percent coverage	100.0 % (req. 100%)	80.13 % (req. 80%)	78.04 %

Table 8 presents the percentage coverage, MRT, and ART obtained by MCLP, MMRT, and MART. Analogously to the previous table, the green colored cells indicate the objective obtained by each formulation. It can be observed that each formulation outperforms the other two with respect to the metric modeled in its corresponding objective function. MCLP provides the theoretical maximum percent coverage achievable by a constellation. Specifically, MCLP obtains 78.04 % percentage coverage while MMRT and MART have 68.98 % and 75.26 %, respectively. Similarly, MMRT and

MART obtain the theoretical minimum MRT and ART, respectively. More precisely, MMRT has an MRT of 15 min, while MCLP and MART have MRTs of 30 min and 25 min, respectively. Furthermore, MART has an ART of 6.96 min, the lowest compared against the 11.66 min and 9.96 min obtained by MCLP and MMRT formulations, respectively. The results presented in this Table enable us to conclude that even though the number of satellites in the constellation is the same, their orbital distribution directly influences the discontinuous coverage metrics. In addition, the results help visualize the independence between the discontinuous coverage metrics, specifically, that improving one metric does not imply improving the remaining ones. Lastly, it is critical to remark how the MMRT sacrifices percentage coverage by breaking the coverage timeline, aiming to reduce the length of the coverage gaps.

Table 8 Comparison between MCLP, MMRT, and MART results.

Metric	MCLP	MMRT	MART
Percent coverage	78.04 %	68.98 %	75.26 %
MRT	30 min	15 min	25 min
ART	11.66 min	9.46 min	6.96 min

B. Set Covering Location Problem Add-Ons

This section aims to provide additional tools to the user by extending the applicability of the formulations presented in Sec. II. The new tools are demonstrated by adopting the SCLP as a baseline.

1. Inter-Satellite Links

SCLP with inter-satellite links (ISL), *i.e.*, max-ISL, determines the minimum cost constellation configuration that satisfies the spatiotemporal coverage requirements (*i.e.*, SCLP), in addition to providing robust ISL during the mission. The link availability between two satellites is encoded in the Boolean parameter $\mathbf{W} \in \{0, 1\}^{T \times J \times J}$, defined as:

$$W_{tjk} = \begin{cases} 1, & \text{if satellite } j \text{ can establish a link with satellite } k \text{ at time step } t \\ 0, & \text{otherwise} \end{cases}$$

In cases where mutual visibility exists, such as with bidirectional ISLs, $W_{tjk} = W_{tkj}$.

In this paper, to obtain W_{tjk} , we denote \mathbf{r}_{tj} and \mathbf{r}_{tk} as the position vectors of satellites j and k at time step t , respectively, and $\boldsymbol{\rho}_{tjk}$ denotes the relative position vector pointing from satellite j to satellite k at time step t . From the argument of geometry as depicted in Fig. 7, the inter-satellite visibility function g_{tjk} is derived as follows:

$$g_{tjk} = (r_{tj}^2 - (R_{\oplus} + \epsilon)^2)^{1/2} + (r_{tk}^2 - (R_{\oplus} + \epsilon)^2)^{1/2} - \rho_{tjk}$$

where $R_{\oplus} = 6378.14$ km is the radius of the Earth, and ϵ is the bias factor to accommodate the additional margin of

altitude (e.g., signal attenuation due to atmosphere). It is intuitive that when $g_{tjk} > 0$, satellite j has visibility over satellite k at time step t . When $g_{tjk} = 0$, ρ_{tjk} is tangential to the sphere defined by the radius of $R_{\oplus} + \epsilon$. Additionally, constraints on the maximum ISL range can be enforced by comparing it against ρ_{tjk} . Note that several symbols (e.g., \mathbf{r}) defined in this section are uniquely defined.

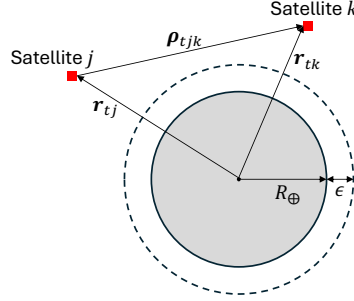


Fig. 7 Geometrical relationship for inter-satellite visibility.

To generate an ISL network topology in which all satellites are connected, we propose leveraging Dirac's theorem [46] to guarantee the existence of a Hamiltonian cycle in the ISL network. Note that a Hamiltonian cycle is a cycle that visits each node exactly once in a graph. To describe Dirac's theorem, we first define, for this section only, the following terms: $V(G)$ represents the set of vertices on a graph G , n is the number of vertices, and $d(q)$ is the degree of vertex $q \in V(G)$.

Theorem 1 (Dirac's Theorem [46]). *Let G be a simple graph with $n \geq 3$, then G is Hamiltonian if $d(q) \geq n/2$ for all $q \in V(G)$.*

In the max-ISL, the set of vertices $V(G)$ is interpreted as the set of orbital slots that form the constellation configuration. The number of vertices equals the number of selected orbital slots, and the degree $d(q)$ of a vertex is interpreted as the number of links that an orbital slot establishes at time step t . We formulate Dirac's theorem with two additional sets of constraints. First, constraint (33a) requires the constellation to have at least three satellites. Second, constraints (33b) enforce that each satellite must have a number of ISLs equal to at least half of the total number of satellites in the constellation.

$$\sum_{j \in \mathcal{J}} x_j \geq 3, \quad (33a)$$

$$\sum_{(j \neq k) \in \mathcal{J}} W_{tjk} x_j - \frac{1}{2} \sum_{j \in \mathcal{J}} x_j \geq 0, \quad \forall t \in \mathcal{T}, \forall k \in \mathcal{J} \quad (33b)$$

The existence of a Hamiltonian cycle for each time step ensures that the network topology is robust in the case of any one satellite failure. The reason is that removing a satellite from the cycle will yield a Hamiltonian path, i.e., a path that visits all the satellites (vertices of the graph). The κ -connectivity of the network is defined as the minimum number of

edges to remove from the graph such that it becomes disconnected. For the resulting network, the k -connectivity (*i.e.*, the minimum number of ISLs required to fail such that at least one satellite is disconnected) is at least $\lceil \frac{1}{2}x \rceil$ and is given by constraints (33b).

Combining the SCLP formulation with Dirac's theorem constraints, the max-ISL formulation is given as:

$$(\text{max-ISL}) \quad \min \quad \sum_{j \in \mathcal{J}} c_j x_j \quad (2)$$

s.t. Constraints (3) and (4)

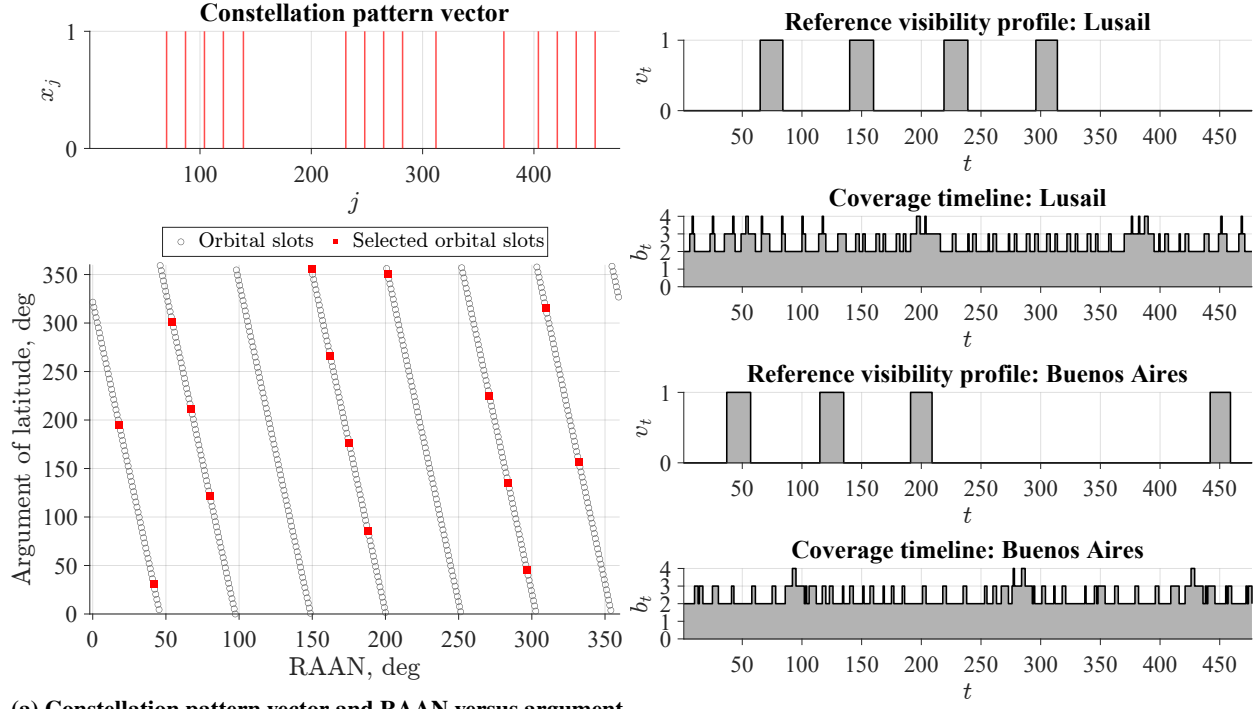
$$\sum_{j \in \mathcal{J}} x_j \geq 3, \quad (33a)$$

$$\sum_{(j \neq k) \in \mathcal{J}} W_{tjk} x_j - \frac{1}{2} \sum_{j \in \mathcal{J}} x_j \geq 0, \quad \forall t \in \mathcal{T}, \forall k \in \mathcal{J} \quad (33b)$$

Example 6 (Robust Communications Constellation Design). We propose an illustrative example that designs a robust satellite constellation for uninterrupted communications between Buenos Aires, Argentina, and Luisal, Qatar, with geodetic coordinates 34.61°S, 58.37°W and 25.50°N, 51.48°E, respectively. For each target, the minimum elevation angle is set to 10 deg, and the coverage requirement r_{tp} is equal to two for all $t \in \mathcal{T}$. The epoch is December 18, 2022, 18:00:00.000 UTC, and the time step size is 180 s. All orbital slots belong to circular RGT orbits with 7:1 resonance, a repetition period of 85,951.43 s, a semi-major axis of 11,507.30 km, and an inclination of 45 deg.

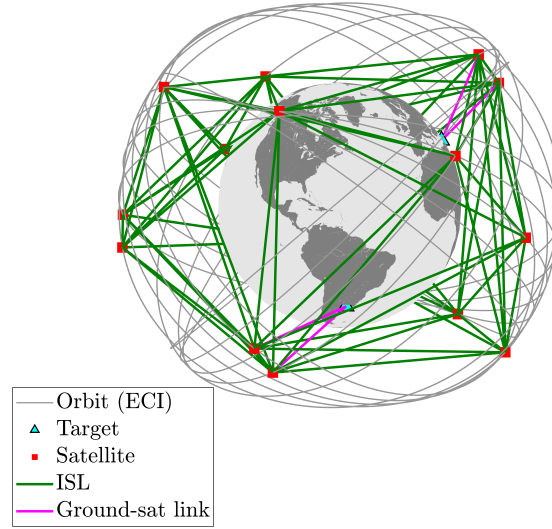
The optimal constellation configuration that delivers continuous two-fold coverage over the ground targets has 15 satellites. Figure 8a outlines the constellation pattern vector and the orbital distribution of the orbital slots in the RAAN versus argument of latitude plane. Further, Fig. 8b shows the reference visibility profile and coverage timeline of the optimal constellation over Luisal and Buenos Aires. Lastly, Fig. 8c illustrates the 3D visualization of the optimal constellation configuration.

To illustrate the robustness of the constellation against a one-satellite failure, we randomly discard one of the satellites. Figure 9 presents the constellation pattern vector, and coverage timelines over Buenos Aires and Luisal before and after removing the satellite located in orbital slot $j = 282$. The coverage drops from a minimum of double-fold to single-fold coverage at specific time steps due to the failure. The constellation is robust in terms of connectivity between satellites and ground stations. The reason for this is that the coverage parameter r_{tp} was defined equal to two for all time steps and all ground stations. Figure 10 presents the network topology for the epoch and time step $t = 105$. The satellites and targets are displayed by projecting them into the 2D geographic map, and the abstract network topology representation is obtained by connecting the satellites with green lines. It is noteworthy to mention that the links are not going through the Earth. The first column of the figure enables the visualization of the impact on the number of connections by randomly removing a satellite, leaving Buenos Aires with a single connection to a satellite. Similarly,



(a) Constellation pattern vector and RAAN versus argument of latitude plots.

(b) Reference visibility and delivered coverage.



(c) 3D visualization of optimal constellation configuration.

Fig. 8 SCLP with ISL formulation results.

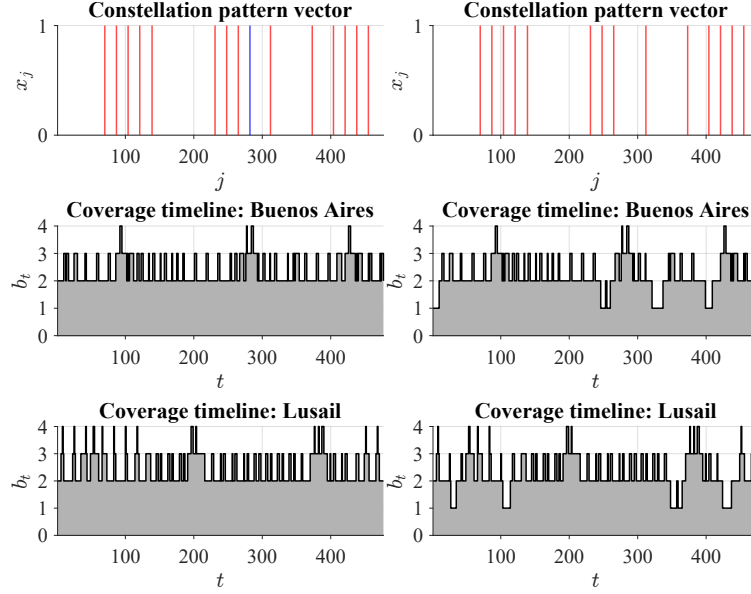


Fig. 9 Constellation pattern vector and coverage timelines before (left) and after (right) one-satellite failure, colored in blue.

the second column of the figure depicts the reduction in ground-to-satellite connections suffered by Luisal at time step $t = 105$ as a consequence of a one-satellite failure.

2. Maximum Revisit Time as a Mission Requirement

In this section, we propose a mathematical formulation to design a minimum cost constellation where the maximum revisit time is a strict constraint. The new formulation adopts SCLP objective function (2), and leverages most of the constraints used in the MRT formulation except for constraints (9), which are dropped. To enforce the MRT as a mission requirement, decision variable Z is recast as parameter z_p , which represents the upper bound on the MRT for target p . Consequently, constraints (17) are replaced by constraints (36). The full formulation is given as:

$$(\text{z-MRT}) \quad \min \quad \sum_{j \in \mathcal{J}} c_j x_j \quad (2)$$

$$\text{s.t.} \quad \text{Constraints (4), (7), (11), (12), (13),} \quad (34)$$

$$(14), (15), (16), \text{ and } (18) \quad (35)$$

$$\omega_{tp} \leq z_p, \quad \forall t \in \mathcal{T}, \forall p \in \mathcal{P} \quad (36)$$

3. Average Revisit Time as a Mission Requirement

This section presents a mathematical optimization formulation to design a minimum cost constellation such that the average revisit time is lower than a user-defined requirement. Objective function (2) is adopted to minimize the cost of

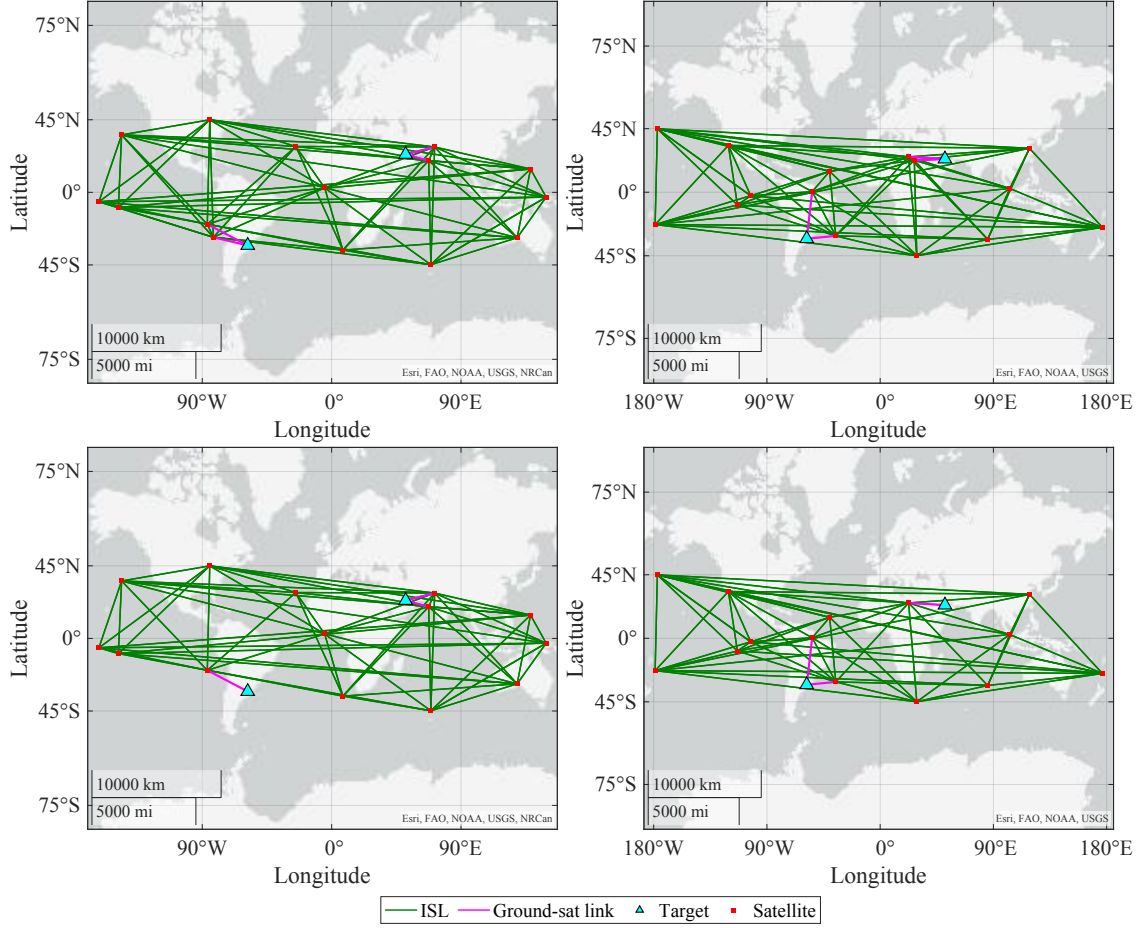


Fig. 10 Satellite and target's projection in the latitude-longitude plane and abstract representation of the network topology at the epoch (left column), and at time step $t = 105$ (right column). The upper and bottom rows display the topology before and after the satellite failure, respectively.

the constellation. From the set of constraints used in Sec. II.G to minimize the ART, we drop cardinality constraints (9) and recast objective function (24) as constraints (39) where γ_p indicates the maximum permissible ART for target p . The full formulation is given as:

$$(\gamma\text{-ART}) \quad \min \quad \sum_{j \in \mathcal{J}} c_j x_j \quad (2)$$

$$\text{s.t.} \quad \text{Constraints (4), (7), (11), (12), (27a), (27b), (27c),} \quad (37)$$

$$(28), (29), (30a), (30b), (30c), \text{ and (31)} \quad (38)$$

$$\alpha_p \leq \gamma_p, \quad \forall p \in \mathcal{P} \quad (39)$$

C. Case Studies

1. Constellation Configuration Design For Space Station Tracking

This case study designs an optimal constellation configuration using PSCLP to provide at least 60 % and 80 % coverage over static and dynamic targets, respectively. The static targets are the three Deep Space Network (DSN) stations located in California, USA, Madrid, Spain, and Canberra, Australia, with coordinates 35.42°N, 116.89°W, 40.43°, 4.24°W, and 35.40°S, 148.98°E, respectively. The dynamic targets considered are the International Space Station (ISS) and the Tiangong Space Station (TSS). The epoch is designated as April 19, 2025, 12:00:00.000 UTC, and the time step size is 120 s. The state vectors of the space stations are determined using MATLAB's built-in function `propagateOrbit` [47]. The TLE information required as input for the function is obtained from CelesTrak [48]. The stations are considered covered if they are in the satellite's line of sight and the range between them is less than 1500 km. For the DSN stations, we define a minimum elevation angle of 15 deg. There are two distinct families of orbital slots corresponding to circular orbits. The first family consists of RGT orbits with 13:1 resonance, period of repetition of 85,254.04 s, altitude of 1200.17 km, and an inclination of 45 deg. The second family, consisting of non-RGT orbits, adopts the same altitude and inclination, but uniformly discretizes the RAAN and argument of latitude between zero and 360 degrees in 30 and 20 steps, respectively.

The optimal constellation configuration has 30 satellites, from which 11 belong to the RGT orbit family and the remaining 19 to the non-RGT orbits. Figure 11 presents the pattern vector and the distribution of the orbital slots in the RAAN versus argument of latitude plane. The formulation places the satellites spanning the 360 deg corresponding to the argument of latitude. Conversely, the formulation selects the orbital planes that have a RAAN similar to the space stations.

The percentage coverage delivered by the constellation is 60.99 %, 61.27 %, and 60.85 % over the DSN stations in California, Madrid, and Canberra, respectively. Further, the constellation delivers 81.41 %, and 80.28 % coverage over

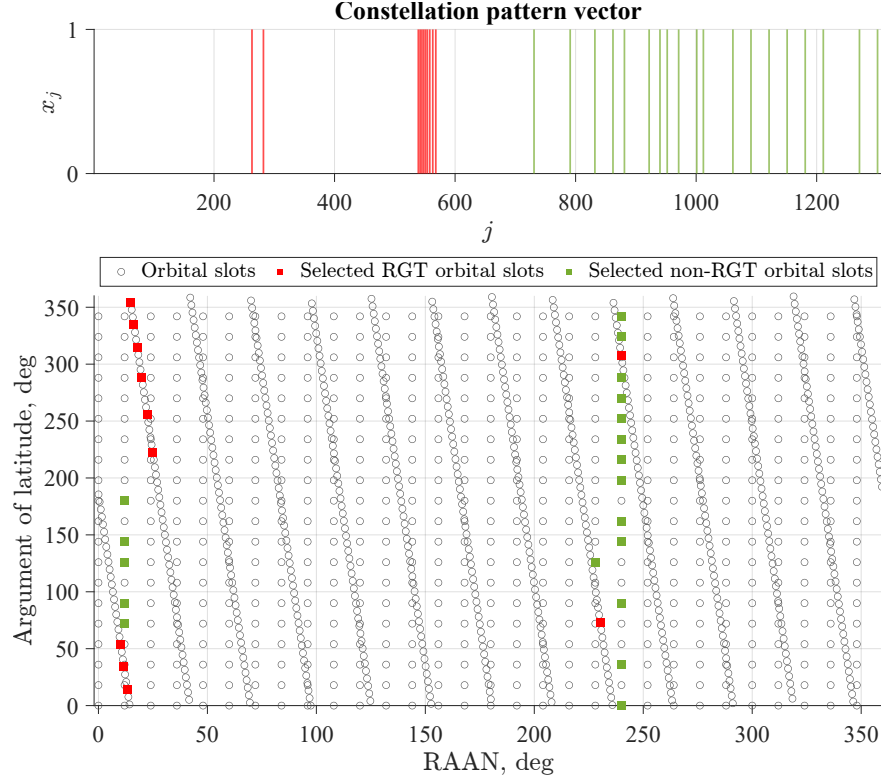


Fig. 11 Optimal constellation configuration's pattern vector and orbital slot distribution.

the ISS and TSS, respectively. Figure 12 outlines the reference visibility profiles of the RGT orbit's seed satellite over the three DSN stations, and the coverage timeline corresponding to the optimal constellation over the DSN and space stations. In addition, Figure 13 shows a 3D visualization of the optimal constellation configuration, the targets, and their orbits at the epoch.

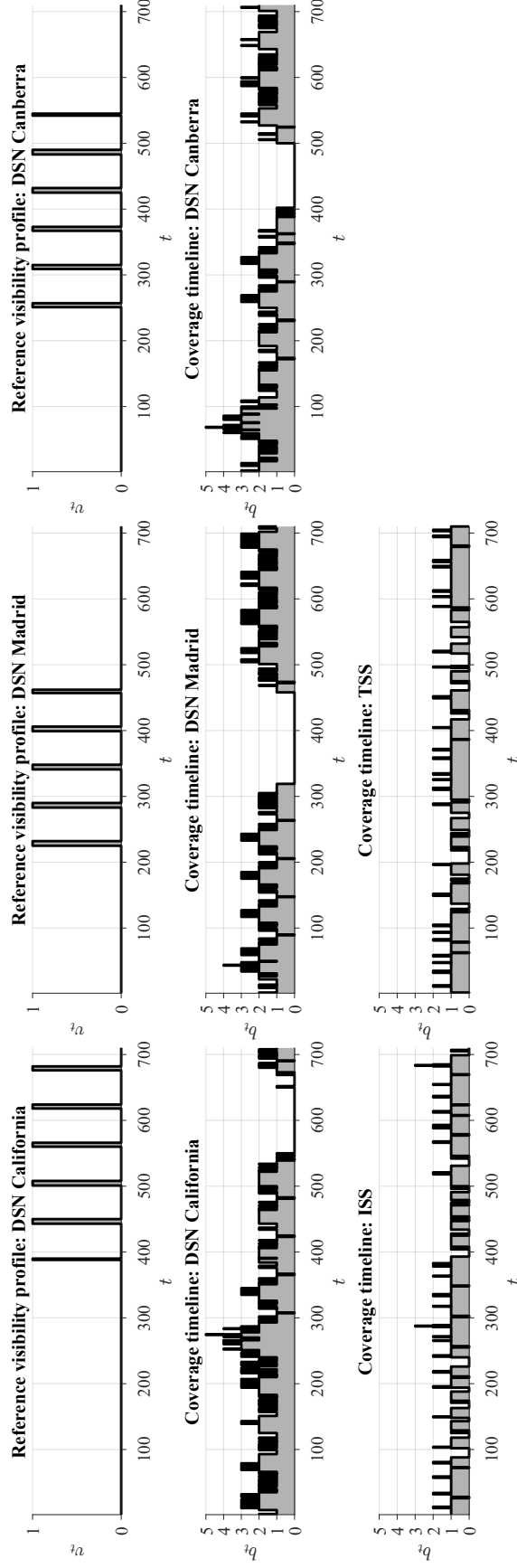


Fig. 12 Reference visibility profiles and coverage timelines for the targets.

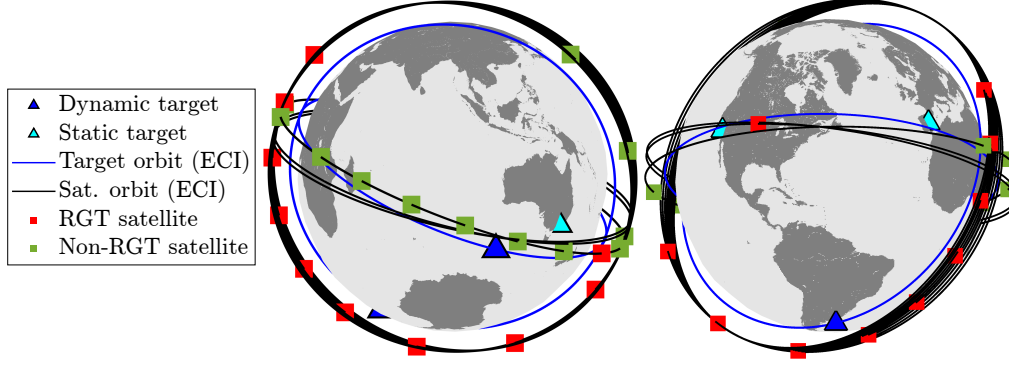


Fig. 13 3D visualization of the optimal constellation at the epoch.

2. SCLP with Deployment Cost

This case study presents the design of a minimum cost constellation configuration to achieve single-fold continuous coverage over Seoul, Republic of Korea, with coordinates 37.55°N, 126.99°E. Specifically, the cost is interpreted as the ΔV required to transfer from the parking orbit to the final orbital slot. The epoch is designated as January 1, 2025, 12:00:00.000 UTC, the time step size is 180 s, and the number of time steps is 1600. The minimum elevation angle is assumed to be 10 deg.

The circular parking orbit is defined with an altitude of 500 km, an inclination of 28.5 deg, a RAAN of 0 deg, and an argument of latitude of 210 deg. For the orbital slots, 154 orbital planes with an altitude of 2000 km are defined from all possible combinations between the candidate RAAN and inclinations. The candidate RAANs are obtained by uniformly discretizing the range between 0 and 360 deg in 14 steps. Similarly, the candidate inclinations encompass the range between 28.5 and 37.55 deg, discretized in 11 intervals. In addition, each orbital plane contains 10 uniformly phased orbital slots.

To determine the cost of each orbital slot, it is assumed that the orbital transfer vehicles (OTV) perform a Homman transfer to achieve an altitude of 2000 km. Subsequently, a change of plane maneuver is performed to arrive in the orbital plane with the corresponding RAAN and inclination. Lastly, phasing maneuvers are performed to cover the orbital plane. It is important to highlight that this case study aims to demonstrate the applicability of SCLP to obtain an optimal constellation configuration given specific transfer costs; consequently, a more efficient concept of operations for the deployment sequence can exist.

The optimal constellation configuration has a cost of 82.52 km/s, and uses 18 satellites. Figure 14a outlines the constellation pattern vector and the coverage timeline. The constellation delivers single, double, and triple-fold coverage over Seoul. Figure 14b presents the cost of selected orbital slots. Conversely, the larger costs represent plane change maneuvers and phasing. The formulation selects high-cost orbital slots, given that they offer longer visibility periods over the target. Figures 14c and 14d show the orbital slots' distribution in the RAAN versus inclination and RAAN

versus argument of latitude planes, respectively. 14 out of 18 orbital slots have simultaneous RAAN and inclination change. Similarly, all orbital slots perform phasing maneuvers, where the orbital slots located in the plane corresponding to 0 deg are the ones that perform the most. Lastly, Figure 14e presents the 3D illustration of the minimum cost constellation configuration.

To determine the weight of the cost parameter c_j in the optimization outcome, we maintain the same set of parameters except for the cost that is set equal to one for all j in \mathcal{J} , and obtain the optimal constellation configuration. Defining the same cost for all satellites yields the constellation configuration that requires the minimum number of satellites to deliver continuous coverage over the target. SCLP retrieves an optimal configuration that uses 17 satellites, one less than the optimal configuration that minimizes the deployment cost. The ΔV required to deploy the new constellation is 95.55 km/s, representing an increase of 15 % with respect to the minimum ΔV required of 82.52 km/s. Figures 15a and 15b present a side-by-side comparison of the costs of the selected orbital slots by the two optimization problems. The new formulation, which is not aware of the costs of orbital slots, selects the ones that contribute the most to achieving continuous coverage over the target; consequently, the selected orbital slots have higher costs than the initially selected ones. Further, Fig. 15c showcases that the new constellation configuration selects upper-right orbital slots, associated with higher ΔV costs.

IV. Conclusions

This paper presents a unified optimization framework, a collection of MILP formulations, to design provably optimal (for a given discrete set of candidate orbits) constellation configurations, considering coverage as the figure of merit. The nature of the formulations enables us to solve the optimization problem using a commercial solver and obtain its certificate of optimality. Each one optimizes the design of the constellation configuration adopting a distinct metric, *i.e.*, continuous coverage, percentage coverage, MRT, and ART. Further, we leverage the modularity of MILP formulations to model new mission requirements by interchanging constraints and objective functions between the core formulations.

Throughout the paper, three sets of experiments are conducted. First, we define a common mission scenario and obtain the optimal constellation configuration using all optimization formulations presented. Second, we perform a comparative study between the previous results and identify the key differences between each formulation. Third, we present a collection of case studies aiming to demonstrate further application scenarios. Specifically, we design an optimal constellation configuration with ISL and robust to at least one satellite failure, an optimal constellation configuration capable of covering the three DSN stations and the two international stations. Lastly, we design a constellation configuration with minimum deployment cost.

This paper serves as a stepping stone for future research directions. First, the add-ons section does not encompass all possible combinations between the set of objective functions and constraints presented herein; hence, further combinations can be explored to enable mission designers to incorporate new mission requirements into the constellation

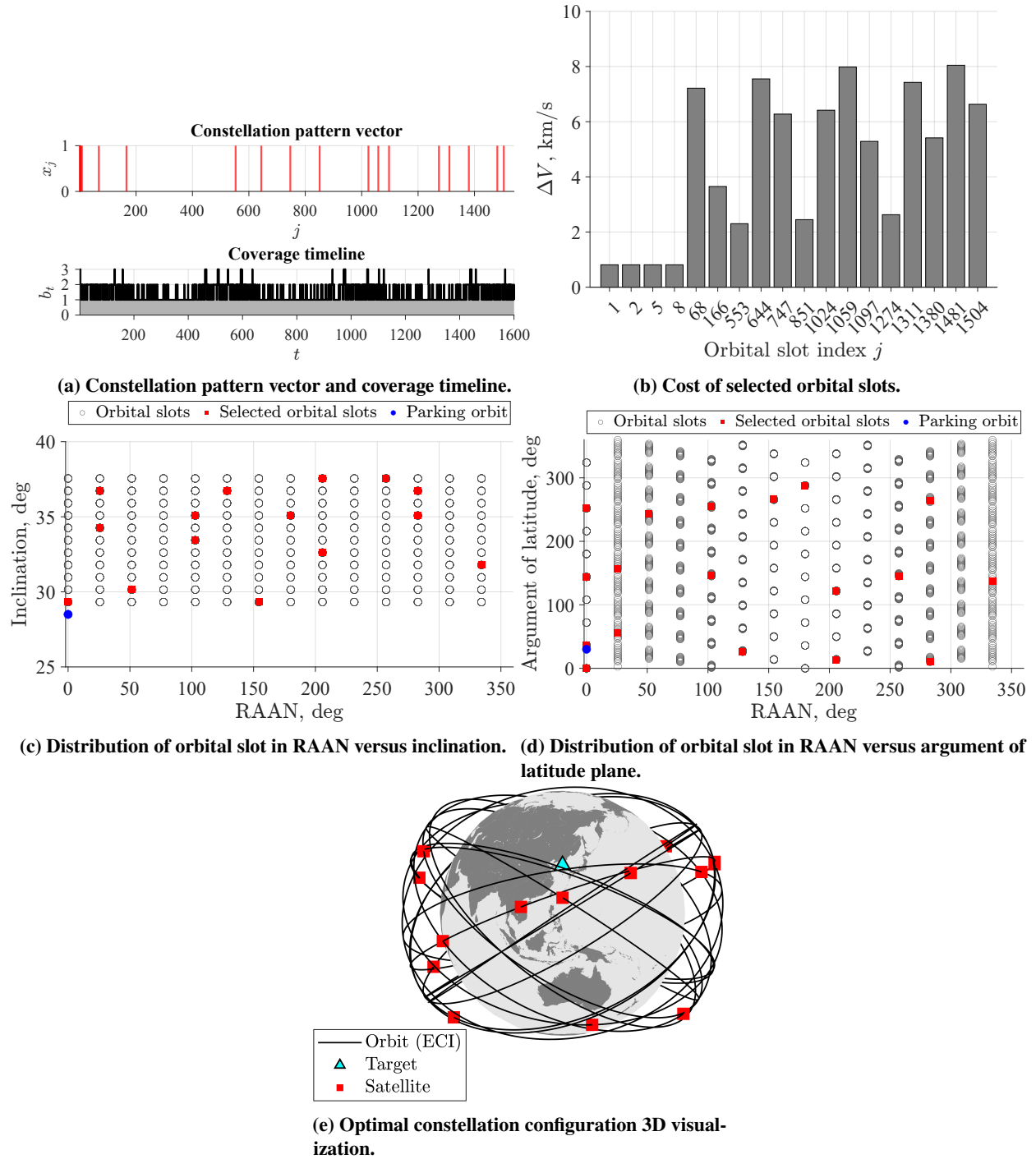
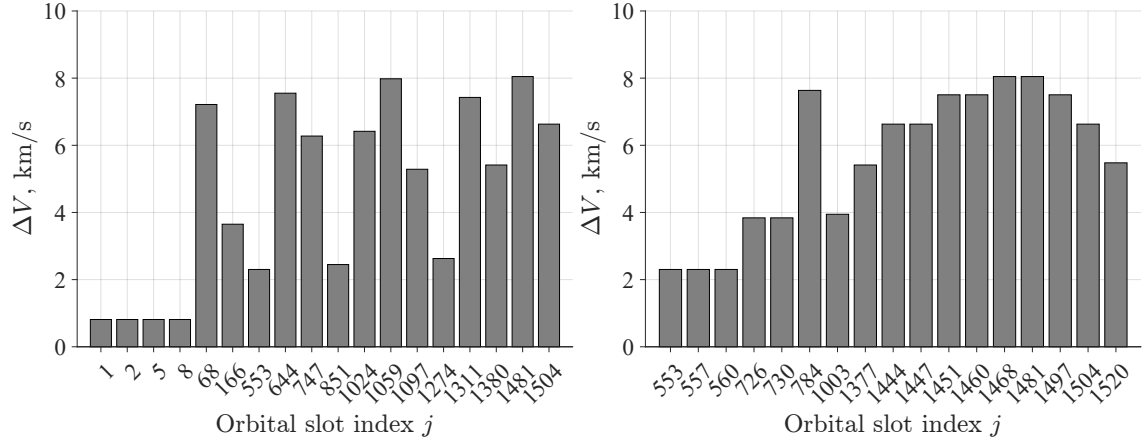


Fig. 14 SCLP with deployment cost results.



○ Orbital slots ■ Selected ΔV informed orbital slots ■ Selected ΔV non-informed orbital slots ● Parking orbit

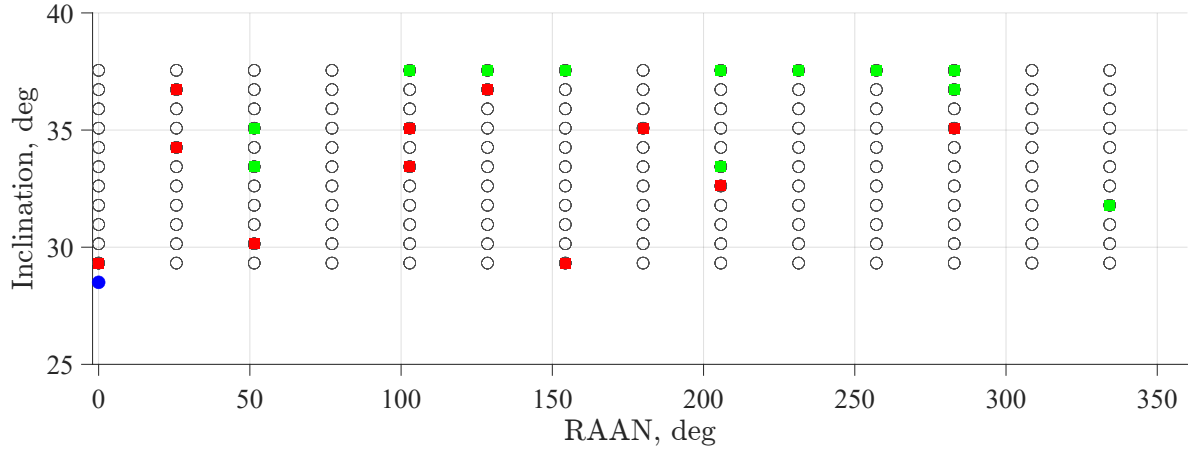


Fig. 15 SCLP with deployment cost orbital parameters distribution for two optimal configurations.

configuration optimization. Second, MILP specific solution methods capable of reducing the computational runtime of the formulations can be investigated.

Acknowledgment

This research is based on work sponsored by TelePIX Co., Ltd.

References

- [1] Stephens, G. L., Vane, D. G., Boain, R. J., Mace, G. G., Sassen, K., Wang, Z., Illingworth, A. J., O’connor, E. J., Rossow, W. B., Durden, S. L., et al., “THE CLOUDSAT MISSION AND THE A-TRAIN: A New Dimension of Space-Based Observations of Clouds and Precipitation,” *Bulletin of the American Meteorological Society*, Vol. 83, No. 12, 2002, pp. 1771–1790. <https://doi.org/10.1175/BAMS-83-12-1771>.
- [2] Paek, S. W., Kronig, L. G., Ivanov, A. B., and de Week, O. L., “Satellite constellation design algorithm for remote sensing of diurnal cycles phenomena,” *Advances in Space Research*, Vol. 62, No. 9, 2018, pp. 2529–2550. <https://doi.org/10.1016/j.asr.2018.07.012>.
- [3] Xue, Y., Li, Y., Guang, J., Zhang, X., and and, J. G., “Small satellite remote sensing and applications – history, current and future,” *International Journal of Remote Sensing*, Vol. 29, No. 15, 2008, pp. 4339–4372. <https://doi.org/10.1080/01431160801914945>.
- [4] Leyva-Mayorga, I., Soret, B., Röper, M., Wübben, D., Matthiesen, B., Dekorsy, A., and Popovski, P., “LEO Small-Satellite Constellations for 5G and Beyond-5G Communications,” *IEEE Access*, Vol. 8, 2020, pp. 184955–184964. <https://doi.org/10.1109/ACCESS.2020.3029620>.
- [5] Kodheli, O., Guidotti, A., and Vanelli-Coralli, A., “Integration of Satellites in 5G through LEO Constellations,” *GLOBECOM 2017 - 2017 IEEE Global Communications Conference*, 2017, pp. 1–6. <https://doi.org/10.1109/GLOCOM.2017.8255103>.
- [6] Evans, B. G., “The role of satellites in 5G,” *2014 7th Advanced Satellite Multimedia Systems Conference and the 13th Signal Processing for Space Communications Workshop (ASMS/SPSC)*, 2014, pp. 197–202. <https://doi.org/10.1109/ASMS-SPSC.2014.6934544>.
- [7] National Coordination Office for Space-Based Positioning, Navigation, and Timing, “Global Positioning System,” <https://www.gps.gov/systems/gps/space/>, 2022. [retrieved 20 May 2025].
- [8] European Space Agency, “GLONASS General Introduction,” https://gssc.esa.int/navipedia/index.php/GLONASS_General_Introduction, 2011. [retrieved 21 May 2025].
- [9] European Space Agency, “What is Galileo?” https://www.esa.int/Applications/Satellite_navigation/Galileo/What_is_Galileo, 2025. [retrieved 21 May 2025].
- [10] Martins, J. R. R. A., and Lambe, A. B., “Multidisciplinary Design Optimization: A Survey of Architectures,” *AIAA Journal*, Vol. 51, No. 9, 2013, pp. 2049–2075. <https://doi.org/10.2514/1.J051895>.

- [11] Jilla, C. D., and Miller, D. W., “Multi-Objective, Multidisciplinary Design Optimization Methodology for Distributed Satellite Systems,” *Journal of Spacecraft and Rockets*, Vol. 41, No. 1, 2004, pp. 39–50. <https://doi.org/10.2514/1.9206>.
- [12] Shi, R., Liu, L., Long, T., Wu, Y., and Wang, G. G., “Multidisciplinary modeling and surrogate assisted optimization for satellite constellation systems,” *Structural and Multidisciplinary Optimization*, Vol. 58, 2018, pp. 1615–1488. <https://doi.org/10.1007/s00158-018-2032-1>.
- [13] Budianto, I. A., and Olds, J. R., “Design and Deployment of a Satellite Constellation Using Collaborative Optimization,” *Journal of Spacecraft and Rockets*, Vol. 41, No. 6, 2004, pp. 956–963. <https://doi.org/10.2514/1.14254>.
- [14] Wertz, J., *Mission Geometry; Orbit and Constellation Design and Management*, Springer Dordrecht, 2002.
- [15] Lee, H., Shimizu, S., Yoshikawa, S., and Ho, K., “Satellite constellation pattern optimization for complex regional coverage,” *Journal of Spacecraft and Rockets*, Vol. 57, No. 6, 2020, pp. 1309–1327. <https://doi.org/10.2514/1.A34657>.
- [16] García, S., and Marín, A., “Covering Location Problems,” *Location Science*, Springer International Publishing, 2015, pp. 93–114. https://doi.org/10.1007/978-3-319-13111-5_5.
- [17] Lee, H., and Ho, K., “Regional Constellation Reconfiguration Problem: Integer Linear Programming Formulation and Lagrangian Heuristic Method,” *Journal of Spacecraft and Rockets*, Vol. 60, No. 6, 2023, pp. 1828–1845. <https://doi.org/10.2514/1.A35685>.
- [18] Church, R., and ReVelle, C., “The maximal covering location problem,” *Papers of the regional science association*, Vol. 32, Springer-Verlag Berlin/Heidelberg, 1974, pp. 101–118. <https://doi.org/10.1111/j.1435-5597.1974.tb00902.x>.
- [19] Walker, J. G., “Circular orbit patterns providing continuous whole Earth coverage,” Tech. rep., Royal Aircraft Establishment, 1970.
- [20] Walker, J. G., “Continuous whole Earth-coverage by circular-orbit satellite patterns,” Tech. rep., Royal Aircraft Establishment, 1977.
- [21] Ballard, A., “Rosette Constellations of Earth Satellites,” *IEEE Transactions on Aerospace and Electronic Systems*, Vol. AES-16, No. 5, 1980, pp. 656–673. <https://doi.org/10.1109/TAES.1980.308932>.
- [22] Luders, R. D., “Satellite Networks for Continuous Zonal Coverage,” *ARS Journal*, Vol. 31, No. 2, 1961, pp. 179–184. <https://doi.org/10.2514/8.5422>.
- [23] Beste, D. C., “Design of Satellite Constellations for Optimal Continuous Coverage,” *IEEE Transactions on Aerospace and Electronic Systems*, Vol. AES-14, No. 3, 1978, pp. 466–473. <https://doi.org/10.1109/TAES.1978.308608>.
- [24] Rider, L., “Optimized polar orbit constellations for redundant earth coverage,” *Journal of the Astronautical Sciences*, Vol. 33, 1985, pp. 147–161.

- [25] Lansard, E., Frayssinhes, E., and Palmade, J.-L., “Global design of satellite constellations: a multi-criteria performance comparison of classical walker patterns and new design patterns” Paper IAF 96.A1.02 presented at the 47th International Astronautical Congress, October 7–11, 1996, Beijing.” *Acta Astronautica*, Vol. 42, No. 9, 1998, pp. 555–564. [https://doi.org/10.1016/S0094-5765\(98\)00043-5](https://doi.org/10.1016/S0094-5765(98)00043-5).
- [26] Avendaño, M. E., Davis, J., and Mortari, D., “The 2-D lattice theory of Flower Constellations,” *Celestial Mechanics and Dynamical Astronomy*, Vol. 116, 2013, pp. 325–337. <https://doi.org/10.1007/s10569-013-9493-8>.
- [27] Davis, J., Avendaño, M. E., and Mortari, D., “The 3-D lattice theory of Flower Constellations,” *Celestial Mechanics and Dynamical Astronomy*, Vol. 116, 2013, p. 339–356. <https://doi.org/10.1007/s10569-013-9494-7>.
- [28] Capez, G. M., Henn, S., Fraire, J. A., and Garello, R., “Sparse Satellite Constellation Design for Global and Regional Direct-to-Satellite IoT Services,” *IEEE Transactions on Aerospace and Electronic Systems*, Vol. 58, No. 5, 2022, pp. 3786–3801. <https://doi.org/10.1109/TAES.2022.3185970>.
- [29] Wang, P., Di, B., and Song, L., “Mega-Constellation Design for Integrated Satellite-Terrestrial Networks for Global Seamless Connectivity,” *IEEE Wireless Communications Letters*, Vol. 11, No. 8, 2022, pp. 1669–1673. <https://doi.org/10.1109/LWC.2022.3171574>.
- [30] Adams, W. S., and Rider, L., “Circular polar constellations providing continuous single or multiple coverage above a specified latitude,” *Journal of the Astronautical Sciences*, Vol. 35, 1987, pp. 155–192.
- [31] Draim, J. E., “Three-and four-satellite continuous-coverage constellations,” *Journal of Guidance, Control, and Dynamics*, Vol. 8, No. 6, 1985, pp. 725–730. <https://doi.org/10.2514/3.20244>.
- [32] Lin, C.-H., and Hong, Z.-C., “Mission and constellation design for low-cost weather observation satellites,” *Journal of spacecraft and rockets*, Vol. 42, No. 1, 2005, pp. 118–123. <https://doi.org/10.2514/1.4652>.
- [33] Ma, D.-M., Hong, Z.-C., Lee, T.-H., and Chang, B.-J., “Design of a micro-satellite constellation for communication,” *Acta Astronautica*, Vol. 82, No. 1, 2013, pp. 54–59. <https://doi.org/10.1016/j.actaastro.2012.04.037>, 6th International Workshop on Satellite Constellation and Formation Flying.
- [34] Ely, T. A., and Lieb, E., “Three-and four-satellite continuous-coverage constellations,” *The Journal of the Astronautical Sciences*, Vol. 54, 2006, pp. 53–67. <https://doi.org/10.1007/BF03256476>.
- [35] Ulybyshev, Y., “Near-polar satellite constellations for continuous global coverage,” *Journal of spacecraft and rockets*, Vol. 36, No. 1, 1999, pp. 92–99. <https://doi.org/10.2514/2.3419>.
- [36] Ulybyshev, Y., “Design of satellite constellations with continuous coverage on elliptic orbits of Molniya type,” *Cosmic Research*, Vol. 47, 2009, p. 310–321. <https://doi.org/10.1134/S0010952509040066>.
- [37] Ulybyshev, Y., “Satellite constellation design for complex coverage,” *Journal of Spacecraft and Rockets*, Vol. 45, No. 4, 2008, pp. 843–849. <https://doi.org/10.2514/1.35369>.

- [38] Bruno, M. J., and Pernicka, H. J., “Tundra constellation design and stationkeeping,” *Journal of spacecraft and rockets*, Vol. 42, No. 5, 2005, pp. 902–912. <https://doi.org/10.2514/1.7765>.
- [39] Meziane-Tani, I., Métris, G., Lion, G., Deschamps, A., Bendimerad, F. T., and Bekhti, M., “Optimization of small satellite constellation design for continuous mutual regional coverage with multi-objective genetic algorithm,” *International Journal of Computational Intelligence Systems*, Vol. 9, No. 4, 2016, pp. 627–637. <https://doi.org/10.1080/18756891.2016.1204112>.
- [40] Chadalavada, P., and Dutta, A., “Regional CubeSat Constellation Design to Monitor Hurricanes,” *IEEE Transactions on Geoscience and Remote Sensing*, Vol. 60, 2022, pp. 1–8. <https://doi.org/10.1109/TGRS.2021.3124473>.
- [41] Mortari, D., De Sanctis, M., and Lucente, M., “Design of Flower Constellations for Telecommunication Services,” *Proceedings of the IEEE*, Vol. 99, No. 11, 2011, pp. 2008–2019. <https://doi.org/10.1109/JPROC.2011.2158766>.
- [42] Ferringer, M. P., and Spencer, D. B., “Satellite constellation design tradeoffs using multiple-objective evolutionary computation,” *Journal of spacecraft and rockets*, Vol. 43, No. 6, 2006, pp. 1404–1411. <https://doi.org/10.2514/1.18788>.
- [43] Williams, E. A., Crossley, W. A., and Lang, T. J., “Average and maximum revisit time trade studies for satellite constellations using a multiobjective genetic algorithm,” *The Journal of the astronautical sciences*, Vol. 49, 2001, pp. 385–400. <https://doi.org/10.1007/BF03546229>.
- [44] Ferringer, M. P., Clifton, R. S., and Thompson, T. G., “Efficient and accurate evolutionary multi-objective optimization paradigms for satellite constellation design,” *Journal of Spacecraft and Rockets*, Vol. 44, No. 3, 2007, pp. 682–691. <https://doi.org/10.2514/1.26747>.
- [45] Wertz, J., Everett, D., and Puschell, J., *Space Mission Engineering: The New SMAD*, Space technology library, Microcosm Press, 2011.
- [46] Li, H., “Generalizations of Dirac’s theorem in Hamiltonian graph theory—A survey,” *Discrete Mathematics*, Vol. 313, No. 19, 2013, pp. 2034–2053. <https://doi.org/10.1016/j.disc.2012.11.025>.
- [47] MATLAB, 23.2.0.2459199 (R2023b) Update 5, The MathWorks Inc., Natick, Massachusetts, 2023.
- [48] Kelso, T., “CelesTrak,” <https://celestrak.org/>, 2025. [retrieved 18 Apr. 2025].